The Canadian Journal of Chemical Engineering

formerly

CANADIAN JOURNAL OF TECHNOLOGY

UNIVERSITY OF MICHIGAN
JUN 2 1959
ENGINEERING LIBRARY

CONTENTS

A Radioactive Tracer Technique for Particle Velocity Measurement in Solids-Gas Systems	*W. H. Gauvin, I. S. Pasternak, L. B. Torobin, L. Yaffe*	95
Principles and Operation of an Air Operated Mixer-Settler	*W. G. Mathers, E. E. Winter*	99
Mixing Efficiency Determinations for Continuous Flow Systems	*A. Cholette, Leonce Cloutier*	105
Sodium Hydroxide-Sodium Sulphate Stripping of Uranium from Amine Extracts	*A. I. Bellingham, R. Simard*	113
A Note on Thermodynamic Consistency of Ternary Vapor-Liquid Equilibrium Data	*James C.M. Li, Benjamin C.-Y. Lu*	117
Some Thermodynamic Properties of the System Formic Acid-Water	*A. C. Plewes, D. C. Pei, R. K. Code*	121
Letters to the Editor	*E. G. Chilton, M. E. Charles, T. W. F. Russell*	127

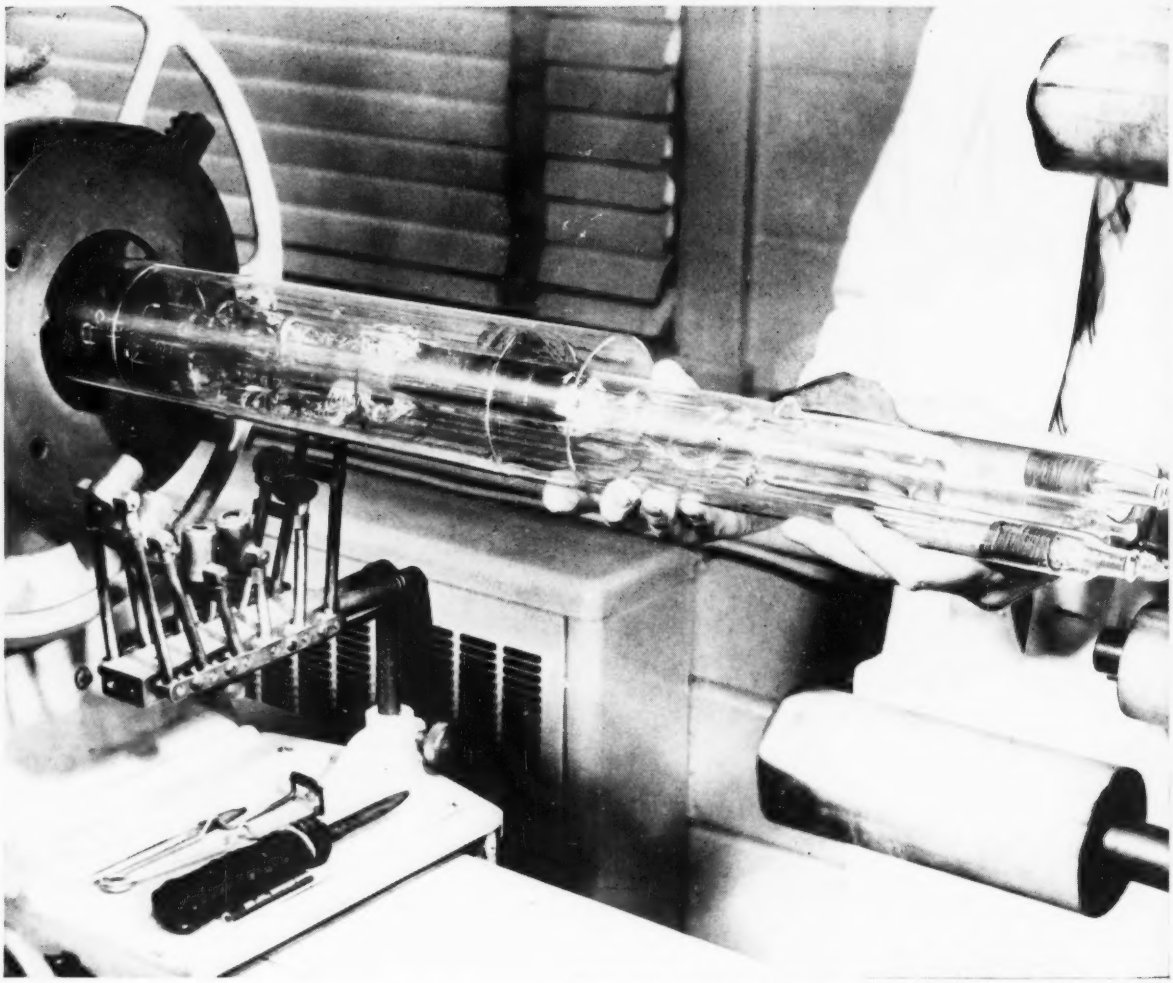

Photograph taken at C-I-L Central Research Laboratory, McMasterville, Que.

POLYMERIC PRECISION

This is an ebulliometer—being assembled by the master glass-blower on his own lathe at our Central Research Laboratory.

The ebulliometer uses two vapor lift pumps such as those found in electric coffee percolators. One circulates a polymer solution while the other circulates boiling solvent—each liquid stream is directed over a temperature detector so sensitive that a difference of one-millionth of 1°C. may be sensed. This device allows the measurement of high molecular weights related to the physical properties of polymers.

Such C-I-L research contributes to higher standards of performance in the plastics industry . . . to new and better plastic products . . . and—through better technical service—to greater success in the application of these new materials to modern living.

C-I-L

CANADIAN INDUSTRIES LIMITED

Serving Canadians Through Chemistry

Agricultural Chemicals • Ammunition • Coated Fabrics • Industrial Chemicals • Commercial Explosives • Paints • Plastics • Textile Fibres

The Canadian Journal of Chemical Engineering

formerly

Canadian Journal of Technology

VOLUME 37 JUNE, 1959 NUMBER 3

Editor
A. Cholette
Faculty of Science, Laval University
Quebec, Que.

Managing Editor
T. H. G. Michael

Publishing Editor
D. W. Emmerson

Assistant Publishing Editors
R. G. Watson
R. N. Callaghan

Circulation Manager
M. M. Lockey

EDITORIAL BOARD

Chairman
W. M. CAMPBELL, Atomic Energy of Canada Limited, Chalk River, Ont.

L. D. DOUGAN, Polymer Corp. Limited, Sarnia, Ont.

W. H. GAUVIN, McGill University, Montreal, Que.

GLEN GAY, Defence Research Board, Ottawa, Ont.

G. W. GOVIER, University of Alberta, Edmonton, Alta.

A. I. JOHNSON, University of Toronto, Toronto, Ont.

E. B. LUSBY, Imperial Oil Limited, Toronto, Ont.

LEO MARION, National Research Council, Ottawa, Ont.

R. R. McLAUGHLIN, University of Toronto, Toronto, Ont.

G. L. OSBERG, National Research Council, Ottawa, Ont.

H. R. L. STREIGHT, Du Pont of Canada Limited, Montreal, Que.

EX-OFFICIO

C. E. CARSON, President, The Chemical Institute of Canada

H. S. SUTHERLAND, Chairman of the Board of Directors

H. BORDEN MARSHALL, Director of Publicity and Publications

W. G. DICKS, Associate Director of Publicity and Publications

Authorized as second class mail, Post Office Department, Ottawa. Printed in Canada

Manuscripts for publication should be submitted to the Editor: Dr. A. Cholette, Faculty of Science, Laval University, Boulevard de l'Entente, Quebec, Que. (Instructions to authors are on the last page).

Editorial, Production and Circulation Offices: 18 Rideau Street, Ottawa 2, Ont.

Advertising Office: C. N. McCuaig, manager of advertising sales, *The Canadian Journal of Chemical Engineering*, Room 601, 217 Bay Street, Toronto, Ont. Telephone—EMpire 3-3871.

Plates and Advertising Copy: Send to *The Canadian Journal of Chemical Engineering*, 18 Rideau Street, Ottawa 2, Ont.

Subscription Rates: In Canada—$3.00 per year and 75c per single copy; U.S. and U.K.—$4.00; Foreign—$4.50.

Change of Address: Advise Circulation Department in advance of change of address, providing old as well as new address. Enclose address label if possible.

The Canadian Journal of Chemical Engineering is published by The Chemical Institute of Canada every two months.

Unless it is specifically stated to the contrary, the Institute assumes no responsibility for the statements and opinions expressed in *The Canadian Journal of Chemical Engineering*. Views expressed in the editorials do not necessarily represent the official position of the Institute.

Cholette Appointed as Editor of C.J.Ch.E.

Albert Cholette, chairman and professor of the Department of Chemical Engineering, Laval University, Quebec City, Que. has been appointed Editor of *The Canadian Journal of Chemical Engineering*. This appointment was announced by H. Borden Marshall, Director of Publications of The Chemical Institute of Canada who publish the Journal.

Dr. Cholette was born in Quebec City in 1918. From 1937-40 he was enrolled in chemistry at Laval University and then he entered chemical engineering at McGill University, Montreal. He graduated from McGill with the degree of B.Eng. (honors) in chemical engineering in 1942. That same year he was awarded the British Association Medal. In 1943, he was granted the S.M. degree in chemical engineering at Massachusetts Institute of Technology. After a year of teaching at Laval, he returned to M.I.T. and obtained the Sc.D. degree in chemical engineering in 1945. Since his graduation, Dr. Cholette has been teaching chemical engineering at Laval University.

Manuscripts for *The Canadian Journal of Chemical Engineering* should be mailed directly to:

Dr. A. Cholette, editor,
The Canadian Journal of Chemical Engineering,
Faculty of Science, Laval University,
Boulevard de l'Entente,
Quebec, Que.

A Radioactive Tracer Technique for Particle Velocity Measurement in Solids-Gas Systems[1]

W. H. GAUVIN[2], *I. S. PASTERNAK*[3], *L. B. TOROBIN*[3] *and L. YAFFE*[4]

To record the velocity history of a particle in complex problems of solid-gas flow with greater accuracy than is possible with existing methods, a technique was developed which in essence consists of following the flight of the particle under test—which has been previously tagged with a suitable gamma-emitting nuclide—by means of Geiger probes placed at predetermined points along the outside surface of the duct or reactor and parallel to its axis. Sharp timing pulses are thus obtained on the screen of a cathode-ray oscilloscope, which permit the estimation of the time elapsed between probe stations to less than 1/1000 second. Complete description of the electronic aspects of the method is given, and details of the particle preparation are outlined.

A brief description is given of the application of the method to the determination of the rate of mass and heat transfer from particles in accelerated motion in a turbulent co-current gas stream and to the study of the effects of the turbulent flow parameters on the drag coefficients of particles in highly turbulent fields.

FUNDAMENTAL studies involving the transfer of heat, mass or momentum from particles entrained in a moving fluid share a common difficulty in that they require an accurate knowledge of the particle velocity history. In addition to being capable of good reproducibility, a suitable technique must allow for measurements to be taken simultaneously at many points in a flow field, which could be over a foot in diameter, without the introduction of any disturbance. Gasterstädt (1) was able to determine the velocity of metal balls moving in a two-inch diameter glass tube by recording the change in inductance which their passage would produce in a coil in contact with the circumference of the tube. This method, however, is limited to systems involving relatively large metallic particles being conveyed in relatively small conduits.

[1]*Manuscript received January 6, 1959.*
[2]*Department of Chemical Engineering, McGill University, Pulp and Paper Research Institute of Canada, Montreal, Que.*
[3]*Department of Chemical Engineering, McGill University, Montreal, Que.*
[4]*Department of Chemistry, McGill University, Montreal, Que.*
Contribution from the Department of Chemical Engineering, McGill University, Montreal, Que.

The triggering of a photoelectric circuit by particles has been commonly employed to obtain the settling velocities of particles in a fluid, but the need for an accurately focussed beam of light limits the method to single-particle studies, performed in transparent tubes of small diameter. An unsuccessful attempt to employ a photoelectric system to obtain the drag coefficients of freely-falling shapes in air has been reported by Barker (2). Ballistics experiments usually involve the perforation by the particle of a fine screen, a practice which would introduce large error in velocity studies at low Mach numbers.

A method frequently employed in fluidized transport and pneumatic conveying experiments involves the instantaneous isolation of a section of the conduit by the simultaneous closing of two slide valves. The solids content of the section is then related to the mean particle velocity in the system. Mitlin (3) has shown that measurements of this type are capable of great error, unless tedious precautions are taken. It would not be applicable to the measurement of velocities in the feeding, acceleration or curved sections of such a system.

High speed cinematography is becoming increasingly popular with the advent of improved equipment. The latter is, however, costly and the analysis of results for non-steady motion is difficult since an individual motion camera, firing perhaps 100 ft. of film, is required for each experimental point. Khudiakow (4) has shown that the method may not be used for single particles less than ¼-in. in diameter and at the same time in tubes larger than 2-in. The system has the further weakness of being limited to transparent conduits. A more extensive survey of particle measurement methods is given in a monograph on solids-gas flow (5).

The authors are at present engaged in a study of particulate behavior in turbulent fields. Two problems in particular require accurate knowledge of the particle velocity: the first is concerned with the determination of the rate of heat and mass transfer to individual shapes moving in accelerated motion through a turbulent co-current air stream, while the second involves a study of the effect of the turbulent flow parameters on the drag coefficients of particles in highly turbulent fields, in both

steady and accelerated motions. The methods of particle velocity measurement previously mentioned were all found to be unsuitable, and an accurate technique giving a relatively complete record of an individual particle history was therefore developed.

Experimental method

In essence, the method consists of following the flight of the particle under test—which has been previously tagged with a suitable gamma-emitting nuclide—by means of Geiger probes placed at predetermined points along the outside surface of the duct and parallel to its axis. As the particle passes each probe it fires the Geiger circuit, producing a sharp timing pulse on the screen of a cathode-ray oscilloscope, to the vertical poles of which the probes are connected in parallel. The distances between pulses, suitably photographed, are referred to a signal produced simultaneously from a pulse generator, and permits the estimation of the time elapsed between probe stations to the nearest 1/1000 second. The results obtained are then plotted on a time-versus-distance graph or analyzed by numerical differentiation methods.

(a) *Probe circuit*

In applying this method, a series of Vic-Tic end window Geiger probes, Model 631-56, equipped with 1B85 counter tubes, were placed alongside the test duct. These were connected in parallel to the vertical poles of a Hewlett-Packard Model 130A cathode ray oscilloscope. The latter has a sensitivity of from 1 mv./cm. to 50 v./cm., and can be operated to sweep times as high as 15 sec./cm.

The pulses from the Geiger circuit, together with the timing signals produced by a Wollensak model WF-311 crystal-calibrated pulse generator, were both recorded on Adox KB-14 35-mm. film as they appeared simultaneously on the screen of the oscilloscope. A typical oscilloscope pattern is given in Figure 1. The fine structure of the pattern, i.e. the fine peak of each pulse, as well as the faint downward timing pulses, may not be easily discerned on the photograph as given; nevertheless, the film is easily read with the aid of a projecting microscope supplied with a calibrated stage.

The complete equipment set-up required for the velocity measurements is shown diagrammatically in Figure 2.

An Atomic Energy of Canada Limited Geiger and scintillation probe monitor, Model AEP 1903-S which had been modified by the authors, supplied the probes—connected in parallel—with their required activation voltage. It is equipped with a counting rate meter which operates from an integrating circuit, indicating the amount of

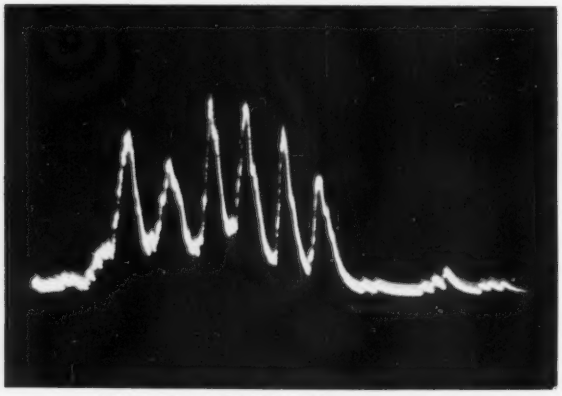

Figure 1—Typical oscillocope pattern.

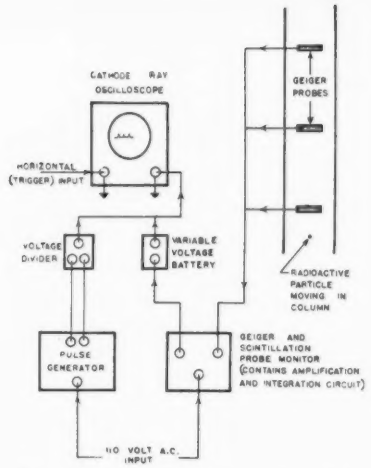

Figure 2—Diagram of velocity measurement equipment.

radiation intercepted by the probes per unit time. This rate increases as the particle approaches a probe, and becomes a maximum when the particle is directly in front of it. The characteristic pulse obtained for a given geometry and particle activation level will vary with the time constant of the integration circuit, and a maximum of pulse definition is obtained by varying its capacitance value. Appropriate capacitors were inserted in the meter circuit to have time constants of 0.8 and 0.08 seconds, the latter being best suited for the particle activation levels employed.

Since the circuit will also detect nuclear events resulting from cosmic radiation and ambient radioactive nuclides, it is necessary to remove this contribution by proper attenuation of the pulse signal. This is accomplished by the inclusion of a variable capacitor into the range selection circuit of the monitor, and also by the proper selection of the oscilloscope amplification level. Capacitors were added to the range circuit so that the instrument could register up to 100,000 counts per minute.

The integrated signal, which had a full scale valve of 40 mv., was taken from a point in the circuit immediately before the meter terminals which was 105 v. above ground level. It was passed through a variable voltage battery pack set to oppose the signal with 105 v., so that only the 40 mv. component carried through to the oscilloscope.

The pulse generator provides a balanced output of approximately one v., and it is reduced to a level of the same order as the integration circuit pulses by means of the voltage divider illustrated in Figure 3. It will allow a calibration pulse height variation of from 0 to 10 mv. A 0.01 micro-farad capacitor has been placed in series with the oscilloscope input to eliminate parasitic back currents.

The relatively inexpensive 1B85 Geiger tubes were found to be quite adequate for the accuracy required in the authors' investigational program. These have, however, a very low efficiency for gamma ray counting (approximately 1%) so that the accuracy of the detection method can be further increased by the substitution of scintillation probes which have efficiencies of up to 100%. These can be fitted with narrow slits and fed into a pulse height analyzer which would reject all pulses, except those which had passed through the slit.

The timing technique described could be replaced by a series of decade counters. Each decade counter, adjusted

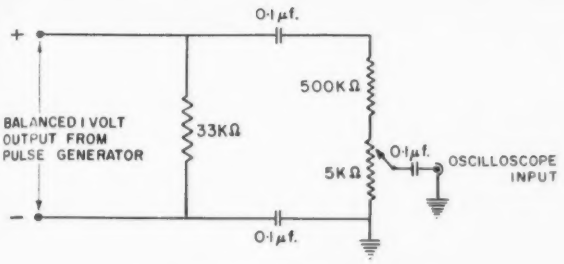

Figure 3—Voltage divider.

to start counting at the peak of a pulse, would operate between two probes, the first pulse opening the timing gate, and the second one closing it. The time interval would be indicated directly on the counter panel, and the time intervals could be given to six figures if desired, provided that the particles were activated to a sufficiently high level.

(b) *Particle preparation*

The minimum particle surface activation level required by the equipment employed and experimental conditions was found to be approximately 20 mr./hr. In the case of celite particles down to ¼-in. in diameter, it was found that this material absorbed sufficient neutrons in a 72-hr. irradiation in the Chalk River N.R.X. reactor in a position having a flux density of 8.6 x 10^{12} neutrons/sec. x $cm.^2$ to bring it to this level.

The natural neutron-absorbing ability of spheres having a wide range of densities and sizes, down to 500 microns in diameter, cannot be relied upon to achieve the required activation level. These spheres were, however, readily prepared in the following manner: Small irregular particles of the desired material (celite, cork or pith have so far been used) were placed in a ball-making apparatus consisting simply of a circular race, two inches in diameter and a half an inch in depth and lined with abrasive strips of varying degrees of roughness. A tangential air jet issuing from a hypodermic needle whirled the particles along the surface of the race, the attrition process shaping them into very accurate spheres in a period generally not exceeding three minutes. The spheres were then soaked in a solution of iridium trichloride and dried under vacuum so that a fraction of a milligram of the salt remained in the interstices of the porous material. The particles were then sprayed with a concentrated solution of DuPont Zytel 61 Nylon resin, and dried at 140°F. for three quarters of an hour. The particles were then restored to accurate sphericity by being re-run in the ball apparatus, operated without an abrasive strip. In this manner the radioactive tracer, when activated, is

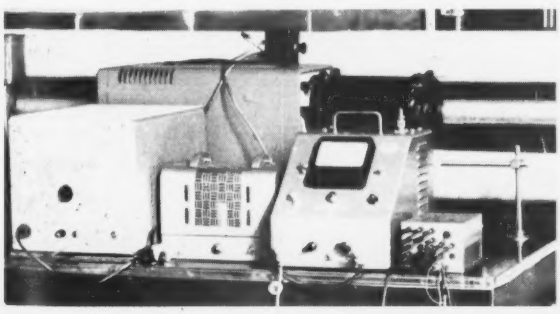

Figure 5—Velocity measuring equipment.

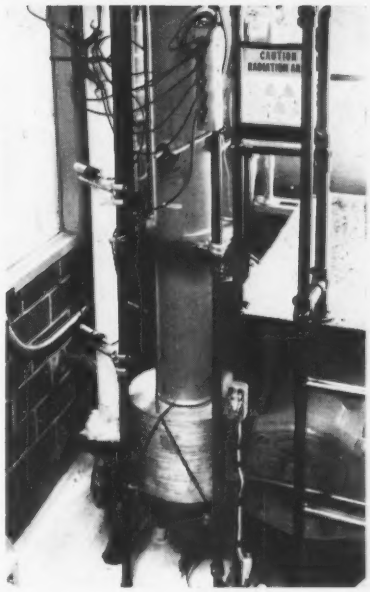

Figure 4—Probes in position along duct surface.

insulated from contact with surfaces which it could contaminate.

(c) *Applications*

The accuracy and reproducibility of the method were intensively tested in connection with the two problems which have already been mentioned. The detailed findings will be discussed in subsequent articles. Only brief descriptions of the experimental procedures will be presented at this time to illustrate typical applications of the velocity measurement method.

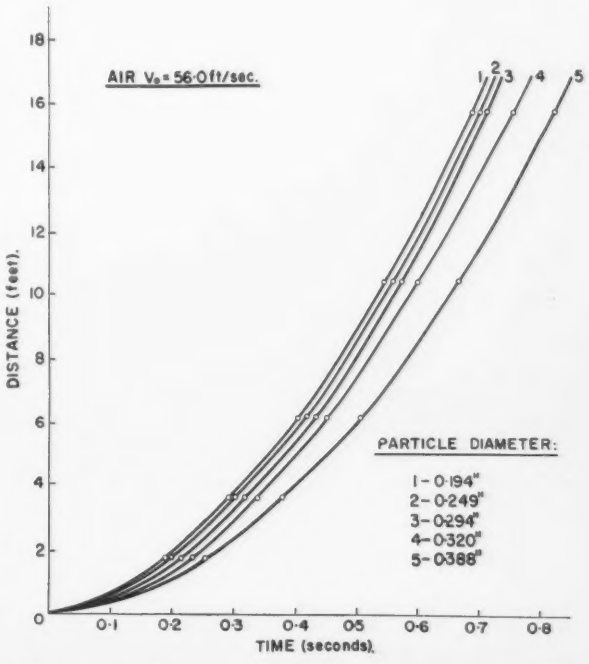

Figure 6 — Time versus distance data for evaporating spheres.

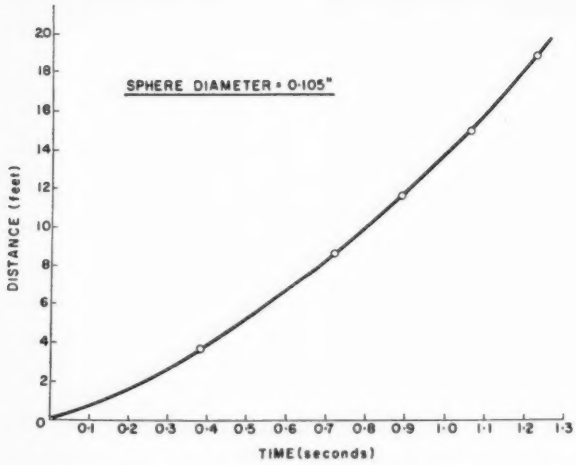

Figure 7—Initial behavior of a sphere falling in a stagnant fluid.

To determine the rate of evaporation in accelerated motion from solid particles wetted with acetone, radioactive celite spheres were dropped vertically from the top of a 1½ in. pyrex glass line, 16-ft. in height, in the presence of a downward co-current turbulent flow of hot air. Seven probes were installed against the outer surface of the insulation covering the glass line, two of which can be seen in position in Figure 4, which shows the lower portion of the mass transfer column, at the left. Not clearly seen is the receptacle containing water, at the bottom of the column, in which the falling sphere is caught, and the unevaporated acetone measured. Figure 5 shows the electronic equipment with the oscilloscope in the back, its screen covered by black bellows to which the camera can be affixed. Shown in front, from left to right, are the pulse generator, the triggering circuit, the Geiger and scintillation probe monitor, containing the amplification and integration circuit, and the variable voltage battery pack. The small black box on top of the oscilloscope houses the voltage divider. Not shown is the triggering device (located on top of the glass column) which starts the sweep of the oscilloscope simultaneously with the release of the particle. Typical of the time-versus-distance data obtained is Figure 6, which describes the particle trajectories for a family of spheres, ranging in size from 0.15-in to 0.39 in., conveyed by air at 410°F. flowing at 56 ft./sec. Interpretation of the complex mass transfer phenomena occurring in such a system could not be attempted if the contact times and continuous velocity history had not been determined.

The second application which is currently being employed is concerned with the effect of high *relative* intensities of turbulence on the drag coefficients of spheres and shapes moving in a turbulent air stream. The spheres are fired singly in a manner which does not impart any rotation to them, through the grid inlet system and along the axis of an 8-in. i.d., 24-ft. high vertical turbulent wind tunnel which has been calibrated for the intensity, scale and spectrum values of the turbulent flow. In this manner, the effect of the turbulence parameters relative to the boundary layer and wake flow of the particle, as well as the effects of various rates of deceleration and acceleration are being studied.

A particle dropping device has also been developed with which the drag on the sphere in the first few moments of flight has been studied, a typical time-versus-distance result of which is given in Figure 7.

All the results so far obtained follow smooth curves without any measurable deviations. No attenuation in sharpness was found when the system was made to correspond to a 12-in. diameter duct surrounded by a 1-in. layer of thermal insulation. The probes can also be placed along any portion of a pipe bend or feeding section so that the average velocity of a multi-particle system can be obtained by the inclusion of a single particle in which a minute radioactive source has been implanted.

It is hoped that the two typical illustrations which have just been discussed will suggest many more such applications for this simple method and thus help to advance the knowledge of the fluid mechanics of solids-gas systems.

References

(1) Gasterstädt, J., Diss. Tech. Hochsch. Dresden (1922).
(2) Barker, D. H., Ph.D. Thesis, University of Utah (1951).
(3) Mitlin, A., Ph.D. Thesis, University of London (1954).
(4) Khudiakow, G. N., Invest. Akad. Navk S.S.S.R., Otdel, Tekh. Navk, 7, 1022-1034 (1953).
(5) Torobin, L. B., and Gauvin, W. H., "Fundamental Properties of Solids-Gas Flow", Pulp and Paper Research Institute of Canada Monograph (1956).

★ ★ ★

Principles and Operation of an Air Operated Mixer-Settler[1]

W. G. MATHERS[2] *and E. E. WINTER*[2]

A mixer-settler for continuous countercurrent solvent extraction is described in which the mixing and pumping of the liquid phases are achieved by air streams.

The operating principles of this mixer-settler are presented in theory and confirmed by experiment. Measurements include interface heights, capacity, air requirements and entrainment of aqueous phase in the solvent under various operating conditions.

The main advantages claimed for this unit are.

1) Mechanical simplicity and consequent freedom from maintenance.

2) Pumps and interface controllers are not required between individual stages.

3) Compactness for a given separation.

4) Low energy requirements.

THE nuclear power reactors to be built in Canada in the near future will be the thermal, heterogeneous type wtih a heavy water moderator and natural uranium fuel. The spent fuel from these reactors will contain plutonium, highly radioactive fission products and uranium. The plutonium is a valuable fuel and will be used in future power reactors, but it will not be used in the first Canadian reactors. Considerable work has been done, however, on processes and equipment to carry out the separations.

At the present time the most economical and versatile process for the recovery and purification of the uranium and plutonium from spent fuel is a solvent extraction process. The highly radioactive nature of the solutions being handled in this process impose certain conditions on the extraction equipment to be used.

(1) It should be essentially maintenance free. Maintenance in a radio chemical plant is difficult and expensive.

(2) It should occupy a relatively small volume for a given throughput and separation duty so as to reduce the amount of shielding.

[1]*Manuscript received October 30, 1958.*
[2]*Atomic Energy of Canada Limited, Chalk River, Ont.*
Contribution from Atomic Energy of Canada Limited, Chalk River, Ont.

(3) A horizontal development is preferable to a vertical one because of the high cost of construction of shielded towers.

At Chalk River emphasis has been placed on an air operated mixer settler known as the airlift contactor. This unit meets the three conditions given above. It is essentially a multi-stage, continuous, counter current, mixer settler in which the mixing and pumping of both phases from stage to stage are carried out by air streams introduced at the bottom of each mixer. Russell and Winter describe the development of an airlift contactor with a nominal uranium processing capacity of 8.5 tons per year (1). The present work describes the design and operation of a three stage air-lift contactor with a nominal processing capacity of 100 tons of uranium per year. In an actual plant each contactor would have to have more than three stages but the data obtained from the three stage unit can easily be extrapolated to larger units.

Although the air lift contactor was developed specifically for reactor fuel processing certain of its features might make it of more general interest. Besides those mentioned above, the power requirements, for the same conditions, are considerably less than those of a mechanically stirred mixer-settler. This will be demonstrated further on in the paper.

Contactor description

A drawing of the three stage contactor is presented in Figure 1. Referring to Figure 1 those chambers containing lift tubes are mixers and the others settlers. In operation, air streams are introduced at the bottom of each mixer and rise through the totally submerged lift tube. A circulation of liquid is thus set up within the mixer and leads to a thorough mixing of the two phases. A schematic diagram of the flow through the contactor appears in Figure 2. In common with all mixer settlers the flow of the two phases is countercurrent between the stages and concurrent in any given stage. The two phases enter a given mixer from opposite directions, are contacted, and then flow into the settler through the mixed phase port. The phases are separated by gravity in the settler and the light phase proceeds to the next mixer through a baffled rectangular weir. The function of the baffle is to minimize a backward flow of mixed phases into the settler by

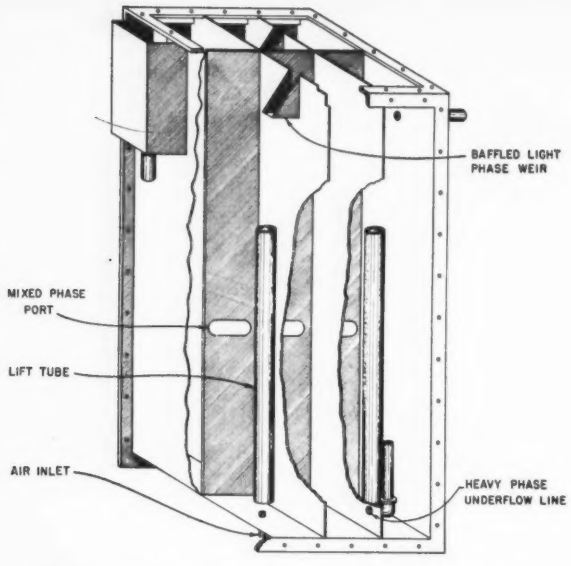

Figure 1—Three stage air lift contactor isometric view.

splashing. The heavy phase proceeds in the opposite direction through an underflow line into the next mixer. Referring to Figure 1 it can be seen that this line rises into the mixer. It will be demonstrated that the height of this riser serves to determine the interface position for a given set of operating conditions.

The experimental contactor was constructed from stainless steel with plates of the transparent plastic Homalite on the front, top and back. Thus visual observation of the contactor operation was possible.

Principles of operation

In a mixer settler with inter stage connections as shown in Figure 2, all liquid levels and interface heights can be determined in terms of known quantities provided the following requirements are met:

(1) The mixing is "perfect", i.e., the ratio of the two phases in a mixer is everywhere the same.

(2) Pressure drops due to flow throughout the apparatus are negligibly small in comparison with various static pressures.

(3) The dynamic pressure which is due to the mixing circulation at the point where the heavy phase enters the mixer and at the mixed phase port must not differ appreciably from the static pressure at those points.

Criterion (2) above is a question of proper design. Whether or not criteria (1) and (3) are satisfied for a particular mixer settler can only be settled by test.

Referring to Figure 2 the total depth of liquid in settler 1 will be uniquely determined by weir geometry and light phase flow rate. The difference in level between settler 1 and mixer 1, Δh_1, can then be determined by an hydraulic balance through the mixed phase port. If the mixing is "perfect" the fluid in the mixer will have an average density given by

$$\rho_{AV,\,1} = f_{H,\,1}\,\rho_{H,\,1} + (1 - f_{H,\,1})\rho_{L,\,1}$$

where f_H is the volume fraction of heavy phase in the mixer.

ρ is the fluid density.

Using this expression the balance through the port gives

$$\Delta h_1 = \frac{\rho_{H,\,1} - \rho_{L,\,1}}{H,\,1 + \left(\dfrac{1 - f_{H,\,1}}{f_{H,\,1}}\right)\rho_{L,\,1}}\,(h_s - h_o) \quad \ldots\ldots\ldots (1)$$

where Δh is the difference in the liquid height between the settler and mixer h_s,h_o refer to heights as shown in Figure 2.

Examination of Equation (1) shows that Δh will always be positive, i.e., in a given stage the total liquid depth in the settler will always be greater than that in the mixer. If Δh_1 is large enough such that the liquid level in mixer 1 lies below the crest of the weir connecting settler 2 and mixer 1 then the flow through this weir will be unimpeded and the total liquid depth in settler 2 will be the same as that in settler 1 since the weir geometries and light phase flow rates are the same for both stages. This argument can be extended to show that, in a multistage contactor provided individual Δh's are large enough, the total liquid depth in all settlers will be the same. Since there is no hydraulic gradient in the settlers it can be seen that the mixing, in effect, pumps the light phase through the contactor. Requiring the liquid depth in a given mixer to be below the crest of the weir emptying into it is equivalent to saying that Δh must be greater than the height of liquid over the weir crest in the settler. Ideally then one could use Equation (1) and the

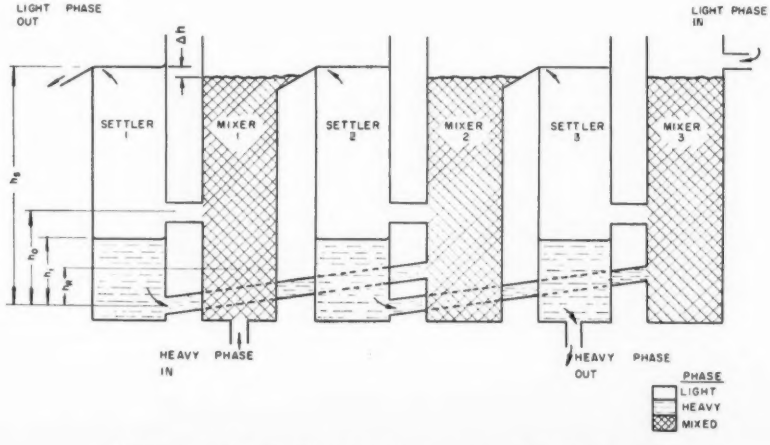

Figure 2 — Schematic flow diagram for the three stage mixer settler.

appropriate weir formula to obtain a crest width which would prevent the appearance of an hydraulic gradient for any given set of operating conditions. In practice, however, the term f_H in Equation (1) may not be known (as will be shown later) and weir formulae breakdown for the small depths considered here so that a considerable safety factor should be incorporated into any such procedure. There is nothing wrong, for instance, with having weirs which are wider than they need be.

It should be mentioned here that Equation (1) will only apply when the interface in each settler lies below the mixed phase port between the mixer and settler. If it should be above this port the liquid depth in the mixer can become greater than that in the settler thus impeding the light phase flow into the mixer. This condition can set up an hydraulic gradient in the contactor. It will be shown below under what condition this can take place in the model under consideration.

To determine the interface height in settler 1 and hydraulic balance is made from settler 1 through the heavy phase underflow line to mixer 2 and through the mixed phase port to settler 2. This gives

$$h_{i,1}\rho_{H,1} + (h_s - h_{i,1})\rho_{L,1} = h_R\rho_{H,1} + (h_o - h_R)(f_{H,2}\rho_{H,2} + (1 - f_{H,2})\rho_{L,2}) + (h_s - h_o)\rho_{L,2} \quad \ldots(2)$$

where

h's refer to heights as shown in Figure 2.

Equation (2) can be rearranged to solve for the interface height and gives:

$$h_{i,1} = h_o f_{H,2}\left[\frac{\rho_{H,2} - \rho_{L,2}}{\rho_{H,1} - \rho_{L,1}}\right] + h_R\left[\frac{\rho_{H,1} - (f_{H,2}\rho_{H,2} + (1 - f_{H,2})\rho_{L,2})}{\rho_{H,1} - \rho_{L,1}}\right] + h_s\left[\frac{\rho_{L,2} - \rho_{L,1}}{\rho_{H,1} - \rho_{L,1}}\right] \quad \ldots(3)$$

Equation (3) is a general expression for interface height for the case where the density of both phases is varying from stage to stage. Some special cases can now be considered.

When there is no density change between stages in either phase Equation (3) becomes

$$h_{i,1} = f_{H,2}h_o + (1 - f_{H,2})h_R \quad \ldots(4)$$

and, in particular, if the stages are connected such that $h_R = O$ then

$$h_{i,1} = f_{H,2}h_o \quad \ldots(5)$$

$f_{H,2}$ will always be between O and 1 so that, in this case, $h_o > h_{i,1} > O$, i.e., the interface lies between the required limits.

In the experimental work that follows the validity of the assumptions leading to Equation (3) were tested in a system where no density changes took place. Equation (4) should then apply.

On examination of Equation (3) it can be seen that the first term on the right hand side will always be positive and the second term will also be positive except for the unusual case where the heavy phase in stage 1 is less dense than the mixed phases in mixer 2. It is very unlikely that this situation would ever be met in practice so the second term on the right hand side of Equation (3) can also be assumed to be always positive. The sign of the third term can be either positive or negative depending on whether the light phase density increases or decreases in the direction of its flow. If the light phase density increases in the direction of light phase flow the third term becomes negative and the interface is lower than it would be in the absence of density change. The interface can be maintained above the heavy phase underflow, however, by a suitable choice of h_R.

A more serious condition can exist if the light phase density decreases in the direction of its flow. Here the interfaces will be high and in some systems could rise above the mixed phase port and cause an hydraulic gradient to appear. When this situation exists h_R would be made equal to zero in order to keep the interfaces as low as possible and by requiring that $h_{i,1} < h_o$ the following inequality is obtained from Equation (3).

$$\rho_{L,2} - \rho_{L,1} < \frac{h_o}{h_s}\left[\rho_{H,1} - \rho_{L,1} - f_{H,2}(\rho_{H,2} - \rho_{L,2})\right]$$

This inequality provides a criterion which must be met if the stages in a multi stage contactor are to be connected as in Figure 2.

In the above material the treatment was carried out for the first and second stages of the contactor but it will be realized that it is just as valid for the n^{th} and $n + 1^{th}$ stages.

The interface height in the settler where the heavy phase leaves the contactor must be controlled externally. In this work an adjustable height weir was used.

Interface level

The validity of the assumptions leading to Equation (3) in which interface height within the contactor is predicted was subjected to test. The heavy phase fed to the contactor was 6% NH_4NO_3 and the light phase was a 20% V/V solution of tributyl phosphate in Soltrol* (20% TBP–Soltrol). There is no density change in this system so that Equation (4), should apply. The interface h_i was measured in settler 2 and the phase ratio in mixer 3 was determined by drawing samples of the mixed phases through sample taps. The results are summarized in Table 1.

TABLE 1

COMPARISON BETWEEN OBSERVED AND CALCULATED INTERFACE HEIGHTS

$h_R = 4.75$ ins., $h_o = 11.5$ ins.

Heavy Phase Flow Rate (l./min.)	Light Phase Flow Rate (l./min.)	Heavy Phase Volume Fraction in Mixer (Measured) f_H	Interface Height h_i (ins.)	
			Obs.	Calc.
0.1	1.0	0.100	5.5	5.43
0.5	1.0	0.265	6.5	6.53
1.0	1.0	0.365	7.25	7.22
2.0	1.0	0.496	8.25	8.11
3.0	1.0	0.590	9.44	8.75
3.5	1.0	0.740	10.62	9.74

This data is in good agreement with the theory except for the two final runs where, at an aqueous flow rate of 3 liters/min. the pressure drop through the underflow line has started to become appreciable.

An important result from the data of Table 1 is the fact that the measured fraction of heavy phase in the mixer departs considerably from the heavy phase fraction of the total flow fed to the mixer. Thus in the second last

*Soltrol is the trade name of kerosene fraction.

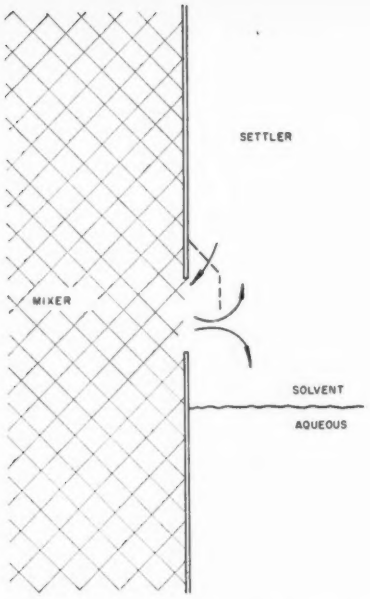

Figure 3—Schematic diagram of the flow pattern between the mixer and settler.

run although 75% of the total feed to the mixer was heavy phase only 59% of the mixed phases in the mixer was heavy phase. If one assumes "perfect" mixing, i.e., no point to point changes in phase ratio within the mixer and a positive flow of the mixed phases through the port into the settler then simple material balance considerations show that at the steady state the volume fraction of heavy phase in the mixer should equal volume fraction of heavy phase fed to the mixer.

The assumption of "perfect" mixing was checked by drawing samples of mixed phases from five different points spaced at intervals between the top and the bottom of the mixer. All five samples showed identical phase ratios so that the assumption of "perfect" mixing is sound. One is therefore forced to the conclusion that there existed a reverse flow of light phase through the upper part of the port connecting the mixer and the settler. This flow pattern is illustrated schematically in Figure 3. If a reverse flow of light phase existed as shown it should be possible to eliminate it almost completely by positioning a baffle where the dashed line appears in Figure 3. This was done while the contactor was in operation and it was observed that the fraction of heavy phase in the mixer increased until it became the same as the fraction fed thus proving the existence of a reverse flow through the unbaffled port. From the design standpoint, then, the term f_H in Equations (1) and (3) will only be known as an upper limit unless the mixed phase port is baffled.

This recirculation of light phase will have the effect of making the light phase retention time in the mixer somewhat greater than that of the heavy phase.

Contactor effectiveness

It has been mentioned above that a solvent extractor for a radiochemical process should occupy a relatively small volume for a given extraction duty and throughput. A relatively low hold up of radioactive solution will serve to reduce both the extent and the thickness of the shielding necessary.

Coplan, Davidson and Zebroski [2] suggest that a measure of extractor compactness which they call contactor effectiveness is given by

$$E_f = \frac{NF}{V}$$

where E_f is the contactor effectiveness
N is the number of theoretical stages for a given system
F is the total flow rate
V is the contactor volume

E_f has the units of reciprocal time and is a direct measure of the relative compactness of a given extractor.

In order to assess the effectiveness of the airlift contactor a run was made in which acetic acid was extracted into hexone (methyl isobutyl ketone). This system was used by Coplan et al to test the KAPL "pump-mix" mixer settler [2] and by Chantry and Berg in a packed column with and without pulsing [3]. Thus a comparison was possible with these three types of extractor.

The conditions of the run are presented in Table 2. In this run the mixer volumes were reduced from 10 liters to 5 liters, using inserts, in order to obtain the same mixer retention time as was used by Coplan et al [2].

TABLE 2

EXTRACTION OF ACETIC ACID INTO HEXONE

Aqueous feed	— 0.969 acetic acid saturated with hexone
Solvent feed	— hexone saturated with water
Aqueous feed rate	— 3.48 liters/min.
Solvent feed rate	— 6.90 liters/min.
Air rate/stage	— 0.30 cfm
Mixer volume	— 5.0 liters
Mixer retention time	— 0.48 mins.
Settler volume	— 10.0 liters

The results of the run are presented as a McCabe-Thiele diagram in Figure 4. The equilibrium curve was obtained by equilibrating samples of the feeds in various volume ratios. The operating line was drawn through the lowest point with a slope equal to aqueous to solvent volume feed ratio.

The data yields an average Murphree stage efficiency (based on aqueous phase analyses) of 93%. Coplan et al report an efficiency of 95 ± 5 for the mechanically stirred "pump-mix" settler with the same mixer retention time and phase ratio. Thus the degree of mixing was comparable in both units.

In Table 3, the effectiveness of the airlift contactor in this run is compared with three other types of extractor.

TABLE 3

COMPARATIVE EFFECTIVENESS OF VARIOUS EXTRACTORS

Extractor	Contactor Effectiveness, E_f* (hours^{-1})
Packed Column (3)	11.7
Pulsed Packed Column (3)	33
Pump-Mix Mixer Settler (2)	27
Air Lift Contractor	39

*A higher value means a smaller volume is required for a given duty.

Too much significance should not be attached to the numerical values in Table 3 since they were arrived at for particular runs and do not necessarily represent maxi-

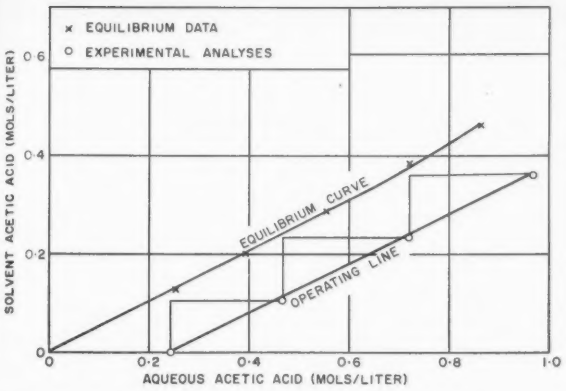

Figure 4—Extraction of acetic acid from water into hexone.

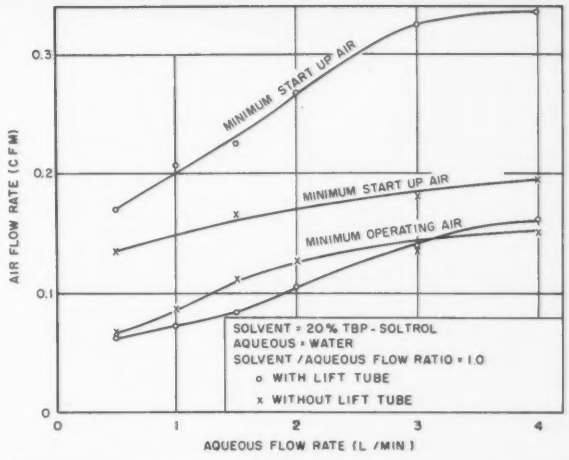

Figure 5—Air flow requirements per stage for various conditions.

mum values for the various units. One can say, however, that pulsing a packed column will reduce the volume necessary for a given duty by a factor of about three and that the pulsed packed column, the "pump-mix" mixer settler and the airlift contactor are close to equivalent in their volume requirements.

Air requirements

An objection to the use of the airlift contactor for the processing of radioactive material is that the air stream leaving the contactors will necessarily contain small amounts of entrained radioactive liquid. If this air is to be discharged to the atmosphere it must first be decontaminated to an acceptable level. It is obvious that this decontamination problem will becomes less severe at lower operating air rates. Consequently it is of interest to know, for a given set of conditions, the minimum air rate which will give satisfactory physical operation of the contactor. The contactor is considered to be operating satisfactorily when the mixers are filled with mixed phases and there exist no point to point changes in phase ratio. This condition was quite easily identified by visual observation.

Some measurements of minimum air flow rates per stage are presented in Figure 5. Water and 20% TBP-Soltrol were fed at a ratio of unity and at varying rates, as shown. It is a peculiarity of the airlift contactor that the minimum air rate required to establish satisfactory operation after an interruption in the air supply has allowed the phases in the mixer to settle (referred to in Figure 5 as a minimum start up air) is less than the air required to maintain proper operation (minimum operating air). The reason for this behaviour is that, on start up, heavy phase only is being pumped through the lift tube. Initially, then the pumping takes place against a certain head. Once proper operation has been established the liquid in the mixer becomes essentially homogeneous as regards density and the pumping head disappears. As a consequence the pumping rate through the lift tube will increase to a value greater than that necessary to maintain good mixing and the air rate can then be reduced without affecting the mixer operation.

Two sets of curves are presented in Figure 5 showing minimum start up of and operating air rates per stage both with the lift tubes in place and with them removed. It can be seen that, while the air required to maintain good mixing is nearly the same in both cases, less air is required to start up when the lift tube is removed. Under these conditions, then, there is some advantage in not using a lift tube. However, when a lift tube is used, a more ordered circulation of liquid within the mixer results. In certain cases this is essential for proper mixer operation. For instance, it has been observed here that, although the 6" x 4" x 26" mixers of the airlift contactor could be operated satisfactorily over a wide range of conditions without lift tubes, when the dimensions were reduced to 6" x 2" x 26", using inserts, the contactor could only be operated with the lift tubes in place.

From the measurements of Figure 5 the magnitude of the air decontamination problem to be expected in a radiochemical process can be evaluated. For instance it can be estimated that, in a plant handling 100 tons of irradiated uranium per year by the TBP process, approximately 2 cubic feet of air per minute will be contacted with highly radio-active liquid. Pilot plant experience in this laboratory has shown that there is no difficulty in decontaminating an air flow of this order to a level well below the tolerable limit [4].

Energy requirements

If the inlet air pressure is known for the data of Figure 5 the energy delivered to the liquid in the mixer can be obtained. This was measured and found to be essentially constant at 1.6 in. Hg. gauge over the range of the data. The energy delivered by this pressure head (the velocity head is negligibly small) in horsepower can then be obtained by multiplying the air rate in cfm by 3.4×10^{-3}.

Referring to Table 2 it can be seen that, in this run, the energy input was 10^{-3} horsepower per stage or 9.6×10^{-5} horsepower per stage per liter/min. of total flow. Overcashier, Kingsley and Olney give a value of 1.5×10^{-3} horsepower per liter/min. of total flow for the same mixer retention time and efficiency in a mechanically stirred mixer [5]. Thus the air lift contactor requires less energy by a factor of 15 for this case.

Aqueous entrainment in the solvent phase

A rough measure of the effect of air flow rate on the interfacial area per unit volume can be obtained by measuring the aqueous entrainment in the solvent stream at varying air rates. This experiment was carried out and the results are presented in Figure 6. The lowest air rate used corresponded to the minimum operating air rate for those conditions. It can be seen that, over the range of the measurements, the amount of entrainment does not depend very greatly on air rate. A possible interpretation of this data is that although an increasing air rate increases

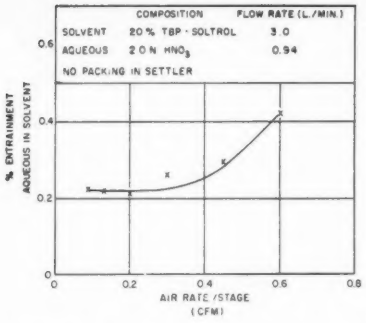
COMPOSITION
FLOW RATE (L./MIN.)
SOLVENT 20% TBP - SOLTROL 3.0
AQUEOUS 2.0 N HNO3 0.94
NO PACKING IN SETTLER
% ENTRAINMENT AQUEOUS IN SOLVENT
AIR RATE /STAGE (CFM)

Figure 6—Effect of air rate on entrainment.

the rate of circulation of liquid within the mixer it does not affect the degree of dispersion of the two phases to any great extent.

Some measurements of aqueous entrainment in the solvent phase as a function of throughput at constant air rate are presented in Figure 7. In the lower curve two sections of York mesh packing were placed in each settler, one above the mixed phase port and one below. In the upper curve no packing was used.

In steady operation a band of unsettled emulsion was observed at the interface. The sharp increase in entrainment at the right hand end of these curves occurred when the top of this band rose to the light phase weirs and overflowed. It can be seen that, with packing, the settler capacity before this point was reached was increased by a factor of three. Also, for a given throughput, the use of packing decreased the amount of entrainment.

Conclusions

The airlift contactor meets the requirements of a solvent extractor for radiochemical processing. Viz:

(1) It is relatively compact and is developed horizontally rather than vertically.

(2) It has no moving parts and consequently requires little or no maintenance.

(3) A multistage unit does not require pumps or interface controllers between the stages.

In addition to the above features the power requirements for a given duty are low in comparison to a mechanically stirred mixer settler. It is also a versatile unit in that it can be operated over a wide range of throughputs and phase ratios.

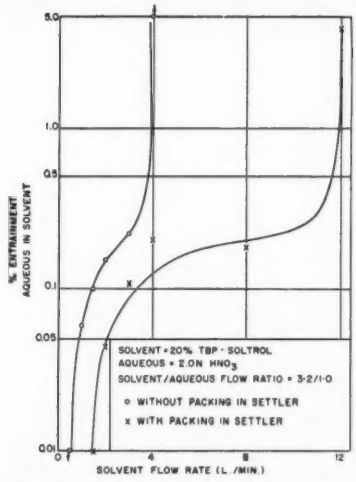
% ENTRAINMENT AQUEOUS IN SOLVENT
SOLVENT FLOW RATE (L./MIN.)
SOLVENT = 20% TBP - SOLTROL
AQUEOUS = 2.0N HNO3
SOLVENT/AQUEOUS FLOW RATIO = 3-2/1-0
o WITHOUT PACKING IN SETTLER
x WITH PACKING IN SETTLER

Figure 7—Effect of flow rate on entrainment.

The chief objection to the use of the airlift contactor in a radiochemical process is the contamination of the air with entrained radioactive liquid. Experience has shown, however, that it is a relatively easy matter to decontaminate the air to a level well below the tolerable limit.

Nomenclature

f is the volume fraction of one of the phases in the mixer
h's are heights as given in Figure 2.
Δh is the difference in liquid height between the settler and the mixer
ρ is the fluid density

Subscripts:

1, 2, 3 refer to stages 1, 2, 3 respectively
H, L refer to the heavy and light phases respectively

References

(1) Russell, S. H., and Winter, E. E., Atomic Energy of Canada Ltd., Report No. CEI-70 (1954).
(2) Coplan, B. V., Davidson, J. K., and Zebroski, E. L., Chem. Eng. Progr. 50, 403 (1954).
(3) Chantry, W. A., Van Berg., R. L., and Wiegandt, Ind. Eng. Chem., 47, 1153 (1955).
(4) Glass, J. Y., and Hoyle, A. C., Atomic Energy of Canada Ltd., Report No. CRCE-666 (1956).
(5) Overcashier, R. H., Kingsley, M. A. Jr., and Olney, R. B., A.I.Ch.E. Journal, 2, 529 (1956).

★ ★ ★

Mixing Efficiency Determinations for Continuous Flow Systems[1]

A. CHOLETTE[2] and LEONCE CLOUTIER[2]

Models are defined for various mixing conditions, in continuous flow systems. Differential equations are derived which take into account an effective volume of mixing, possible short-circuiting, hold-up time of the system, partial displacement or piston flow.

The values of the different factors contained in the integrated equations can be determined experimentally by the particular response of a given system to a sudden change in composition of the feed.

A correlation of the effective volume of mixing and the agitator r.p.m. is presented.

A design procedure is suggested for tank flow reactors when partial mixing occurs.

Les auteurs définissent des modèles pour différentes conditions d'agitation dans les systèmes à écoulement continu. Ils déduisent des équations différentielles qui tiennent compte d'un volume efficace d'agitation, de court-circuits possibles, du temps de rétention du système et de l'écoulement par déplacement ou "frontal".

Les valeurs des différents facteurs contenus dans les équations intégrées peuvent être obtenues à partir de la réponse particulière d'un système donné à un changement subit de la composition de l'alimentation.

Les auteurs présentent une corrélation entre le volume efficace d'agitation et la vitesse de l'agitateur.

Ils proposent une méthode de calcul pour les réacteurs en régime continu lorsque l'agitation est partielle.

MIXING, which has been referred to as one of the most intractable of all the unit operations of chemical engineering [1], has been the object of more and more fundamental work over the past years, partly perhaps on account of the recognized complexity of the subject [2]. Many of the investigations in this field have dealt with batch systems and with the power requirements for mixing [3, 4, 5, 6]. The ever increasing conversion to continuous-flow processes in the industry has introduced various other aspects to the problem for others to explore. Among the numerous avenues of approach followed, a few can be found dealing with the efficiency of mixing. In spite of all the work done in this particular field, much more remains to be accomplished as indicated in recent chemical engineering works [1, 2, 7].

The present investigation was undertaken with the purpose of providing a theoretical basis for evaluating the performance of mixers. The method developed for measuring mixing efficiencies applies to continuous-flow systems but it is intended to extend it to batch systems as well. After presenting a quantitative treatment of various factors likely to be encountered in actual mixing, an experimental study relating to part of the theoretical investigation is exposed.

Previous work

MacMullin and Weber [8] were among the first to present an analytical study of the behavior of perfectly mixed systems, for continuous-flow mixing vessels in series. They, and others [9, 10], used the term "short-circuit" or "mathematical by-passing" to denote conditions involving probability considerations, applicable to well agitated tanks in which the contents are substantially homogeneous, whereby some of the molecules in the feed stream appear almost immediately in the effluent as a result of good agitation. This may be confusing because, as pointed out by Colburn [11], the term "short-circuit" should refer rather to the flow pattern in a tank where some of the feed is channeled to the outlet, reaching the latter without being mixed. It later occurred to MacMullin [12] that short-cut or channelized flow between inlet and outlet would indeed alter conditions in a tank. He suggested, rather qualitatively, that it could perhaps be possible to evaluate the efficiency of a stirrer by studying the conversion rate of a reacting system whose kinetics are known.

Statistical methods have been suggested to determine blending efficiencies [13] for batches of varying concentration fed into a stirred tank.

Danckwerts [14] has introduced the concepts of 'hold-back' and 'segregation' in order to compare actual to ideal mixing conditions in continuous flow systems. The concept of hold-back relates to the residence time of various elements in the system; the author cautions: "the whole F-diagram (and possibly other information) is needed if the actual performance of the reactor is to be calculated". The notion of real 'short-circuit' is mentioned but none of the F diagrams shown take it into account. As to the concept of 'segregation', also obtained from F-diagrams, it is introduced to give an indication of the efficiency of mixing in a system. While it points to the degree of departure of a system from perfect mixing, it does not indicate fully how the system actually behaves. The H and S values thus defined involve rather tedious determinations besides being questionable as to their real advantage.

[1]*Manuscript received January 2, 1959.*
[2]*Department of Chemical Engineering, Laval University, Quebec, Que.*
Contribution from the Department of Chemical Engineering, Laval University, Quebec, Que.
Based on a paper presented at the Joint A.I.Ch.E.-C.I.C. Chemical Engineering Conference, Montreal, Que., April 20-23, 1958.

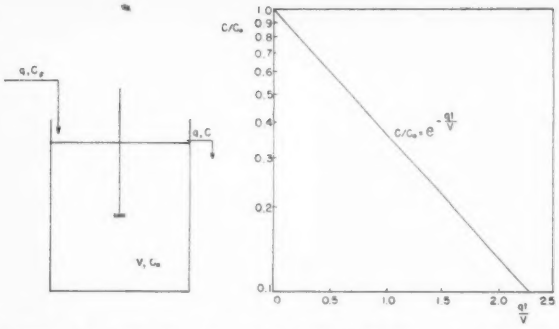

Figure 1—Perfect mixing: the feed is dispersed instantaneously. The composition of the outlet stream is the same as that of the tank contents.

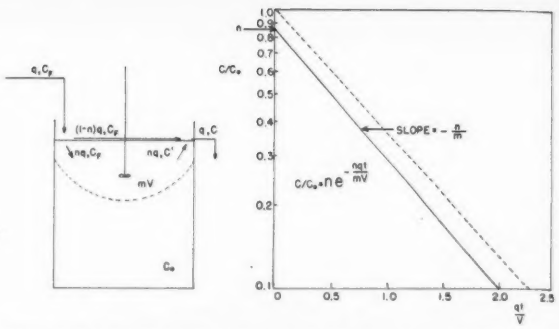

Figure 2—Partial mixing and short-circuit: a fraction of the total volume is perfectly mixed; part of the feed goes directly to the outlet.

Factors involved

With two miscible liquids, in a batch process, a perfectly homogeneous mixture can be obtained when agitation, with the help of diffusion if necessary, is maintained for a long enough period of time. In a continuous flow system, however, it may be that perfect mixing can never be attained. There can be stagnant regions in the reservoir, part of the feed may go directly to the outlet, piston or plug flow may take place. In order to study the behavior of such a system and the efficiency of mixing, one can consider the tank or reservoir to act as a damper to variations in feed composition. The mathematical treatment of this problem thus becomes similar to one performed on a capacity in a servo-mechanism circuit, where a transfer function exists, from which can be obtained transient or permanent responses.

Three factors that may be met in actual mixing conditions are taken into account.

(a) **Effective volume**

For a given agitator, part only of the total tank contents may be well mixed the rest being taken up by stationary or stagnant zones. That part of the total volume where mixing is complete will be referred to as the 'Effective Volume of Mixing': it is the part which acts as a damper to any variation in feed composition and which is considered in determining the transfer function. A somewhat similar concept has been used by Germain [15] for evaluating contact time in a tubular reactor: the author replaces the reactor volume, in which the temperature is variable and passes through a maximum of T_m, by a smaller 'equivalent volume' in which the temperature is uniform, at T_m.

MacDonald and Piret [16] have observed qualitatively that dead volume can retain solution for indeterminate periods of time within a vessel. Danckwerts [14] also considered dead space in a mixing tank when introducing the concept of hold-back.

(b) **Short-circuit**

Depending on the relative position of the inlet with respect to the outlet, part of the feed may go directly to the latter without being mixed, causing channeling or a short-circuit. Only the remaining portion is thus available for mixing. This situation is unlike that arising from the definitions of short-circuit introduced by some authors as mentioned already.

MacDonald and Piret [16] report that they have observed channeling, in the course of experimental determinations, especially at low levels of agitation.

(c) **Piston flow**

In many systems, depending on conditions, part of the feed, or all of it, may give rise to piston or plug flow. Inasmuch as the liquids in the stagnant and well agitated zones are not separated by a membrane, fluctuations or circulation may arise. Liquid in the stagnant zone may be replaced by some from the well agitated zone or from part of the feed. Such a circulation may go on steadily in the form of piston or plug flow.

Nagata and others [17, 18, 19] have studied mixing in a tubular reactor where piston flow exists, but in the absence of any short-circuit.

Mixing problems met in actual practice may involve different combinations of these three factors: effective volume, short-circuit, piston flow. Some particular combinations, more likely perhaps to be encountered than others, will now be considered.

Theory

As for a servomechanism element, the behavior of a mixing system can be studied by means of the answer to either a step, a linear or a harmonic demand. One only of the answers being necessary to determine a transfer function, the first or step demand has been chosen on technical grounds suggested by the experimental determinations to be made. For the different systems considered, the following are the answers to a negative step demand.

1. **Perfect mixing**

The contents of a reservoir, Figure 1, occupy a volume of V cubic feet; the initial concentration is c_o lbs./ft.^{3}. q cu. ft./hr., of composition c_F, are assumed to be fed continuously into the reservoir. The feed composition c_F is changed suddenly at time t = O from c_o to O, creating a step demand. At any given time t, mixing being perfect, the tank contents are uniform throughout and of composition c, which is also that of the effluent.

A material balance for a time element dt gives:

$$qc_F dt = qcdt + d(Vc) \quad \ldots\ldots\ldots\ldots\ldots\ldots (1)$$

The feed composition, c_F, being then zero, and the volume of the liquid in the reservoir being constant, Equation (1) can be written:

$$\frac{dc}{dt} + \frac{q}{V} c = O$$

Upon integration one obtains:

$$c/c_o = e^{-\frac{q}{V}t}$$

When plotted on semi-log paper, as in Figure 1, this equation gives a straight line.

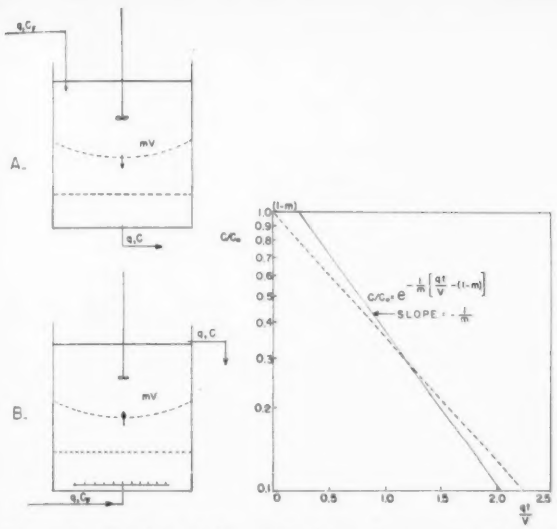

Figure 3—Partial mixing and piston flow: a fraction of the total volume is perfectly agitated; piston flow takes place before or after mixing, as shown.

2. Partial mixing and short-circuit

As shown in Figure 2, only a fraction m of the total volume is assumed to be well agitated. A fraction n of the feed enters the zone of perfect mixing while the other fraction (1 − n) is assumed to be short-circuited directly to the outlet. The concentration, at time t, in the zone of perfect mixing is assumed to be c′. The material issuing from this zone is mixed with that portion of the feed which short-circuits the system, the mixture of the two giving a liquid of composition c at the outlet. One thus obtains:

$$nqc_F dt = nqc'dt + mVdc'$$

or,

$$\frac{dc'}{dt} + \frac{nq}{mV}c' = O$$

$$\therefore\ c'/c_o = e^{-\frac{nq}{mV}t} \qquad \ldots\ldots\ldots\ldots\ldots\ldots (2)$$

But,

$$(1-n)qc_F dt + nqc'dt = qcdt$$

and,

$$c_F = O \therefore\ c = nc'$$

Equation (2) then becomes:

$$c/c_o = ne^{-\frac{nq}{mV}t}$$

Taking natural logarithms:

$$\ln c/c_o = \ln n - \frac{nq}{mV}t$$

Thus, plotting c/c_o vs qt/V on semi-log paper as in Figure 2, the value of n can be read directly on the concentration ratio axis, at t = O. The straight line has a slope of − n/m, from which can be derived the value of m, once n has been determined.

3. Partial mixing and piston flow

With a fraction m of the total volume well agitated, the feed can be considered to give piston flow in two different ways, as shown in Figure 3:

(a) The feed is introduced into the zone of perfect mixing, displacing an equal volume into the stagnant zone: this liquid, in turn, displaces the other already present, by the mechanism of piston or plug flow.

(b) The feed, introduced into the stagnant zone, displaces an equal volume from the latter into the zone of perfect mixing which, in turn, supplies an equivalent volume of liquid to the outlet.

In either case, the composition of the liquid at the outlet would remain constant at c_o for a period of time t = (1 − m) V/q, which represents the time required to displace all the material out of the stagnant zone at the prevalent rate of flow. The variation of the outlet composition with time, in either case, is obtained in the following way:

$$qc_F dt = qc'dt + mVdc'$$

$$\frac{dc'}{dt} + \frac{q}{mV}c' = O$$

$$c'/c_o = e^{-\frac{q}{mV}t}$$

But, c = c′ at time: $t - \frac{(1-m)V}{q}$

$$\therefore\ c/c_o = e^{-\frac{1}{m}\left[\frac{qt}{V} - (1-m)\right]}$$

$$\ln c/c_o = -\frac{1}{m}\left[\frac{qt}{V} - (1-m)\right]$$

Plotting this equation on semi-log paper gives a straight line of slope − 1/m, as shown in Figure 3. The value of m can also be obtained from the intercept at $c/c_o = 1$.

4. Partial mixing with piston flow and short-circuit

Among the several possible combinations, the following three have been considered.

(A) In addition to having a fraction m of the total volume well mixed and a fraction n of the feed going to the zone of perfect mixing, a fraction p of the feed gets into the stagnant zone from where it displaces an equivalent volume by piston flow into the zone of perfect mixing, as shown in Figure 4. The outgoing liquid, of composition c at time t, is made up in part of liquid of composition c′ from the zone of perfect mixing, and of the fraction (1 − n − p) of the feed which short-circuits the tank. Two periods have to be considered, before and after time t = (1 − m) V/p q, during which all the liquid originally in the stagnant zone is displaced.

a) $O < t < (1-m)V/pq$

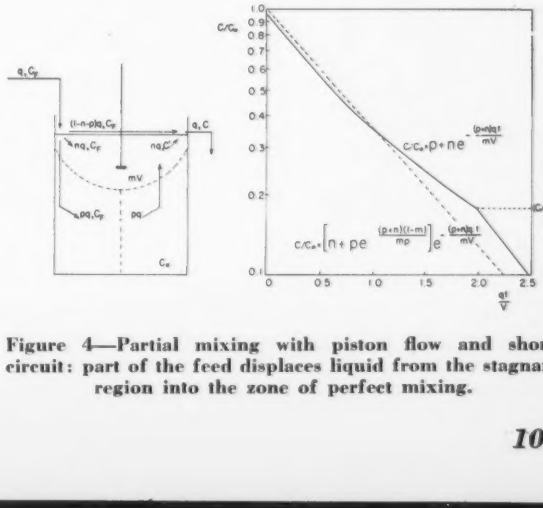

Figure 4—Partial mixing with piston flow and short-circuit: part of the feed displaces liquid from the stagnant region into the zone of perfect mixing.

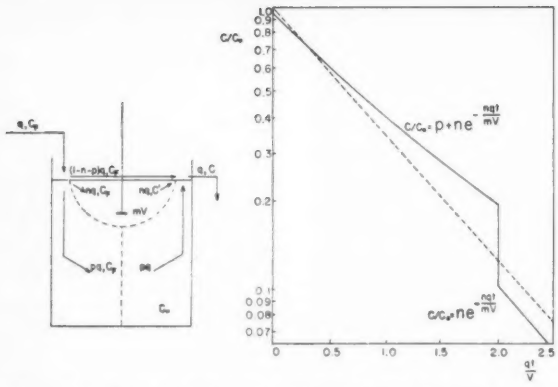

Figure 5—Partial mixing with piston flow and short-circuit: part of the feed displaces liquid from the stagnant region, around the zone of perfect mixing.

During this period, material of composition $c_F = c_o$ enters the zone of perfect mixing from the stagnant zone. The following relations are obtained:

$$nqc_F dt + pqc_o dt = (p + n)\, qc'dt + mVdc'$$

$$\frac{dc'}{dt} + \frac{(p + n)\, q}{mV} c' = \frac{pqc_o}{mV}$$

$$c'/c_o = \frac{p}{p + n} + Ke^{-\frac{(p + n)\, q}{mV} t}$$

Since

$$c' = c_o \text{ at } t = O, \quad K = \frac{n}{p + n}$$

$$c'/c_o = \frac{p}{p + n} + \frac{n}{p + n} e^{-\frac{(p + n)\, q}{mV} t}$$

$$c = (p + n)\, c'$$

$$\therefore c/c_o = p + ne^{-\frac{(p + n)\, q}{mV} t}$$

b) $t > (1 - m)\, V/pq$

All the material originally in the stagnant zone has now left and liquid of composition $c_F = O$ enters the zone of perfect mixing from the stagnant one.

$$\frac{dc'}{dt} + \frac{(p + n)\, q}{mV} c' = O$$

$$c' = K_1' e^{-\frac{(p + n)\, q}{mV} t}$$

$$c/c_o = K_1 e^{-\frac{(p + n)\, q}{mV} t}$$

Now, at time: $t = \dfrac{(1 - m)\, V}{pq}$

$$c/c_o = K_1 e^{-\frac{(p + n)(1 - m)}{mp}} = p + ne^{-\frac{(p + n)(1 - m)}{mp}}$$

$$\therefore K_1 = n + pe^{\frac{(p + n)(1 - m)}{mp}}$$

$$c/c_o = \left[n + pe^{\frac{(p + n)(1 - m)}{mp}}\right] e^{-\frac{(p + n)\, q}{mV} t}$$

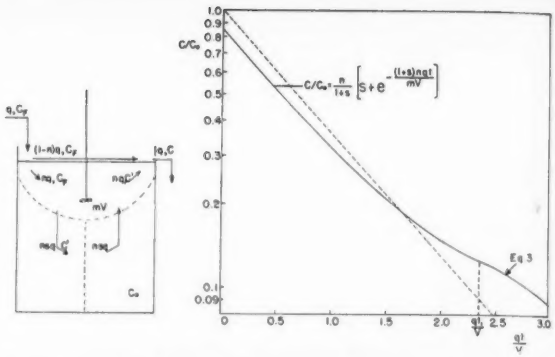

Figure 6—Partial mixing with piston flow and short-circuit: liquid from the zone of perfect mixing displaces, and is replaced by, an equal volume from the stagnant region.

Plotting c/c_o vs qt/V on semi-log paper, for the two regions of case A, gives curves such as shown in Figure 4.

(B) Part of the feed goes to the stagnant zone and displaces an equal volume by piston flow around the zone of perfect mixing, directly to the outlet, as indicated in Figure 5. The outgoing material is made up in part by this stream, in part by liquid forced out of the zone of perfect mixing and also by the part of the feed going in short-circuit.

Again, two periods have to be considered, before and after time: $t = \dfrac{(1 - m)\, V}{pq}$

a) $O < t < \dfrac{(1 - m)\, V}{pq}$

$$nqc_F dt = nqc'dt + mVdc'$$

$$\frac{dc'}{dt} + \frac{nq}{mV} c' = O$$

$$c'/c_o = e^{-\frac{nq}{mV} t}$$

But,

$$c = nc' + pc_o$$

$$\therefore c/c_o = p + ne^{-\frac{nq}{mV} t}$$

b) $t > \dfrac{(1 - m)\, V}{pq}$

$$c'/c_o = e^{-\frac{nq}{mV} t}$$

Now,

$$c = nc'$$

$$\therefore c/c_o = ne^{-\frac{nq}{mV} t}$$

Curves of c/c_o vs qt/V on semi-log paper, for these cases, are as shown in Fig. 5.

(C) A certain amount of liquid, corresponding to a fraction s of that part of the feed which enters the zone of perfect mixing, passes out of the latter into the stagnant zone. As a result an equal volume is displaced, in piston flow, from the stagnant section into the zone of perfect mixing, as shown in Figure 6.

The two periods to be considered are before and after time: $t = \frac{(1 - m)\,V}{nsq}$

a) $O < t < \frac{(1 - m)\,V}{nsq}$

Throughout this time period, liquid of composition c_o is displaced into the zone of perfect mixing from the stagnant one.

$$nqc_F dt + nsqc_o dt = nsqc'dt + nqc'dt + mVdc'$$

$$\frac{dc'}{dt} + \frac{nq}{mV}(1 + s)\,c' = \frac{nsqc_o}{mV}$$

$$c'/c_o = \frac{s}{s + 1} + K_2 e^{-\frac{nq}{mV}(s + 1)\,t}$$

Since $c' = c_o$ at time $t = O$

$$K_2 = \frac{1}{s + 1}$$

Also, $c = nc'$

$$\therefore\ c/c_o = \frac{n}{s + 1}\left[s + e^{-\frac{nq}{mV}(s + 1)\,t}\right]$$

b) $t > \frac{(1 - m)\,V}{nsq}$

Liquid entering the zone of perfect mixing now has the composition c' of the liquid displaced from the zone of perfect mixing into the stagnant one, at time: $t - \frac{(1 - m)\,V}{nsq}$ or, at $t - t_1$.

$$nqc_F dt + nsqc'_{(t - t_1)}\,dt = nsqc'dt + nqc'dt + mVdc'$$

$$\frac{dc'}{dt} + \frac{nq}{mV}(s + 1)c' = \frac{c_o nsq}{(s + 1)mV}\left[s + e^{-\frac{nq}{mV}(s + 1)\left(t - \frac{(1 - m)V}{nsq}\right)}\right]$$

$$c'/c_o = \frac{s^2}{(s + 1)^2} + \frac{nsqt}{(s + 1)_m V} e^{\frac{(s + 1)(1 - m)}{sm} - \frac{nq}{mV}(s + 1)\,t} + K_3 e^{-\frac{nq}{mV}(s + 1)\,t}$$

$$K_3 = \frac{1}{s + 1} + \left[\frac{s}{(s + 1)^2} - \frac{1 - m}{m(s + 1)}\right] e^{\frac{(s + 1)(1 - m)}{sm}}$$

$$c/c_o = \frac{ns^2}{(1 + s)^2} + \frac{n}{1 + s}\left[1 + \left(\frac{s}{1 + s} - \frac{1 - m}{m} + \frac{nsqt}{mV}\right) e^{\frac{(1 + s)(1 - m)}{sm}}\right] e^{-\frac{nq}{mV}(1 + s)\,t} \quad \ldots(3)$$

Curves for the last two cases are shown in Figure 6.

5. Design procedure for tank flow reactors when partial mixing occurs

As pointed out by Smith [20], design procedures for tank flow reactors are still unavailable when partial mixing occurs. The problem may now be solved, in general, by introducing the concepts already mentioned.

For the particular case of partial mixing and short-circuit, as shown in Figure 7, under steady-state flow conditions, the incoming solution has a composition c_F, that in the zone of perfect mixing is c', and the outgoing liquid has a composition c.

A material balance at the outlet gives:

$$(1 - n)\,qc_F + nqc' = qc$$

$$\text{or, } c = (1 - n)\,c_F + nc' \quad \ldots(4)$$

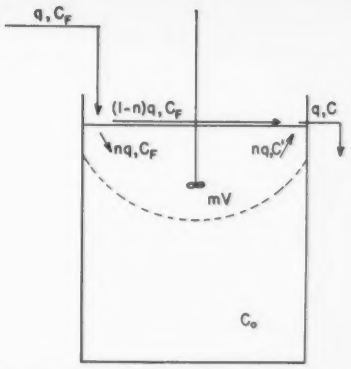

Figure 7—Partial mixing and short-circuit in a chemical reactor.

Now, taking account of the reactant in the feed and exit streams as well as that converted in the reactor, one can write [20]:

$$nqc_F - nqc' = r'mV \quad \ldots(5)$$

where: r' = reaction rate, lbs./(ft.^{3}) (hr.), in the zone of perfect mixing.

mV = actual volume of liquid undergoing reaction.

Equation (5) can be rewritten:

$$c' = c_F - \frac{r'mV}{nq}$$

Introducing this value of c' in Equation (4) gives:

$$c = c_F - \frac{r'mV}{q} \quad \ldots(6)$$

If mixing was perfect in the entire reactor, the concentration of the effluent would be c_M and related to c_F by the following:

$$c_F - c_M = \frac{rV}{q} \quad \ldots(7)$$

where: r = theoretical reaction rate, lbs./(ft.^{3})(hr.), based on concentration c_M.

Combining Equations (6) and (7) gives:

$$c = c_F - m\,(c_F - c_M)\frac{r'}{r}$$

$$m = \left(\frac{c_F - c}{c_F - c_M}\right)\frac{r}{r'} \quad \ldots(8)$$

While Equation (8) is a general solution for partial mixing and short-circuit, many particular solutions can

be obtained depending on the order of the reaction taking place.

Of all the possible solutions, only the following two are considered here:

a) *Zero-order reaction with partial mixing and short-circuit.*

For such a reaction, the rate is independent of concentration, so that $r = r'$.

Then, Equation (8) becomes:

$$m = \frac{c_F - c}{c_F - c_M}$$

Thus, one could either obtain the value of c for a given value of m or determine the effective volume by measuring feed and outlet concentrations and calculating the theoretical outlet composition. It is to be noted that in this case the short-circuit effect cancels out.

b) *First-order reaction, with partial mixing and no short-circuit.*

In a first-order reaction the rate is proportional to the concentration of the reactant. If the concentrations were c_M and c', the reaction rates would be respectively:

$$r = kc_M$$

$$r' = kc'$$

Substituting in Equation (8), one obtains:

$$m = \left(\frac{c_F - c}{c_F - c_M}\right)\frac{c_M}{c'}$$

Now, introducing the value of c' given in Equation (4),

$$m = n\left(\frac{c_F - c}{c_F - c_M}\right)\left(\frac{c_M}{nc_F - c_F + c}\right) \quad \ldots\ldots\ldots\ldots (9)$$

Since the case considered here is that where no short-circuit is present, $n = 1$ and Equation (9) becomes:

$$m = \frac{c_F - c}{c} \cdot \frac{c_M}{c_F - c_M}$$

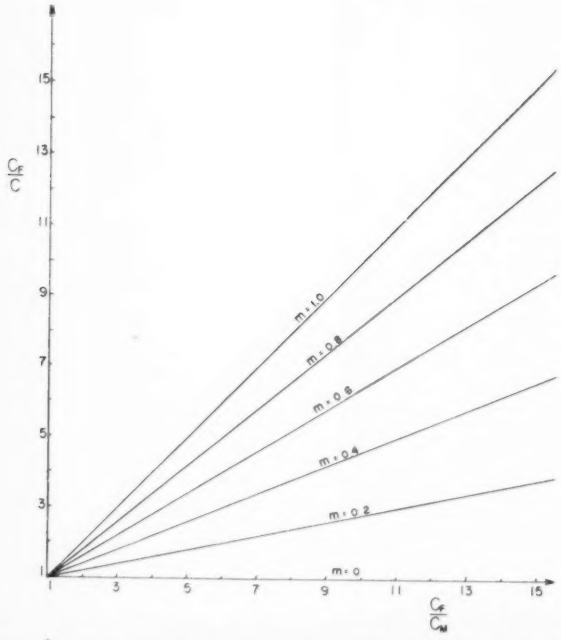

Figure 8—Relation between actual and theoretical outlet concentrations for tank flow reactors when partial mixing occurs.

which can be re-written:

$$\frac{c_F}{c} = m\left(\frac{c_F}{c_M}\right) + (1 - m)$$

The value of $\frac{c_F}{c}$ can be obtained easily from the above expression, or from Figure 8, for given values of $\frac{c_F}{c_M}$ and m.

The designer is thus in a position to predict the performance of a tank-flow reactor.

For cases where short-circuit is present, where higher order reactions are involved or where there is piston flow, studies are actually under way which will be the object of a future publication.

Apparatus

Of the different cases studied theoretically, that involving partial mixing and short-circuit, as described in case No. 2, seemed to be of more immediate interest from an experimental point of view. An apparatus was set up, as shown in Figure 9, in which could be studied simultaneously the variations of effective volume and short-circuit with the level of agitation.

The tank used had an internal diameter of 30". A liquid depth of 30" was assured by a properly located outlet of $\frac{3}{4}$" pipe. The agitator was an experimental model by Chemineer, a $2\frac{1}{2}$" simple turbine with inclined blades being used. A flow regulator and a rotameter were inserted in the $\frac{3}{4}$" feed line. The feed inlet was 12" from the surface of the liquid and the agitator itself was placed in between, at a distance of 6" from the surface.

The agitator speed could be adjusted at the proper value through a variable speed reducer.

Experimental procedure

At the beginning of a run the reservoir was filled to the appropriate level with a solution of NaCl, approximately 1/20 N. After running the agitator for some time at the desired speed to allow for the mixing pattern to be fully developed, water was introduced suddenly at the required rate of approximately 1.15 gallons/min.

Samples were taken at regular time intervals of five minutes and the NaCl concentration determined volumetrically with $AgNO_3$, using K_2CrO_4 as indicator.

Results

The experimental results obtained were plotted, as suggested already, on semi-log paper. Figure 10 shows the

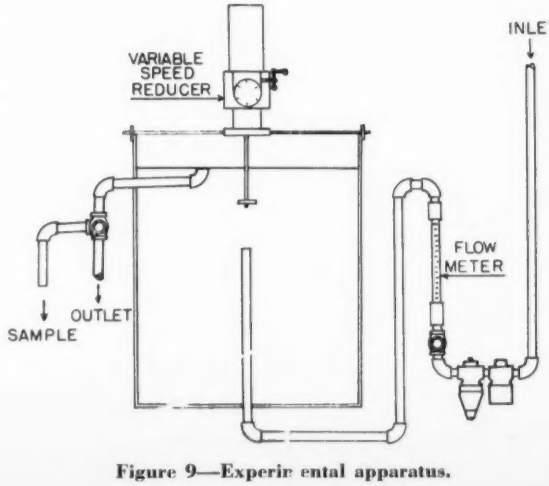

Figure 9—Experir ental apparatus.

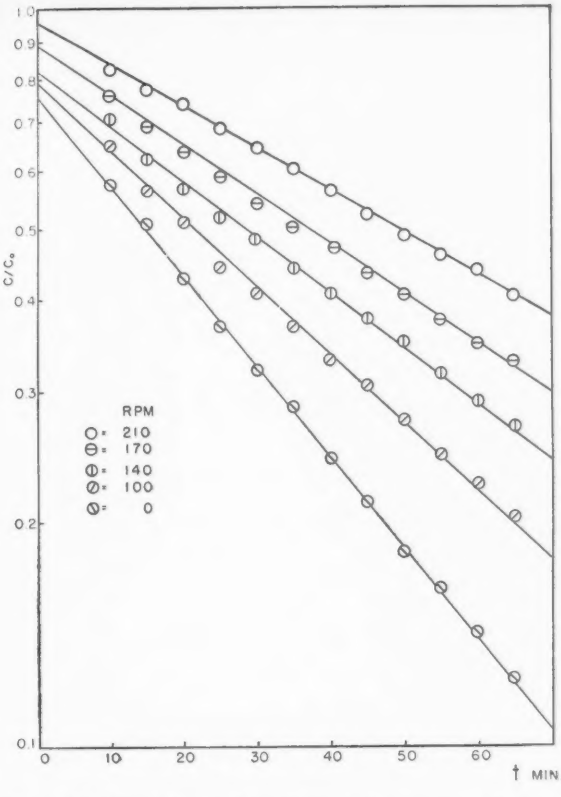

Figure 10—Experimental results: relative concentration vs. time.

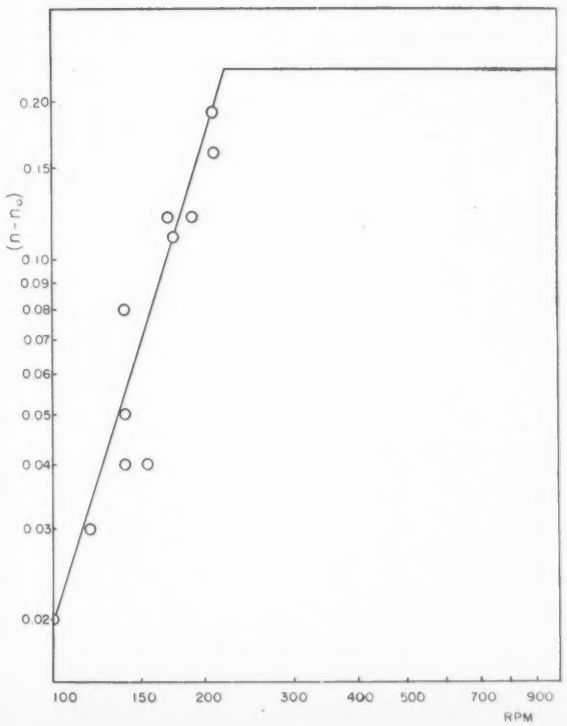

Figure 12—Short-circuit effect vs. agitator speed.

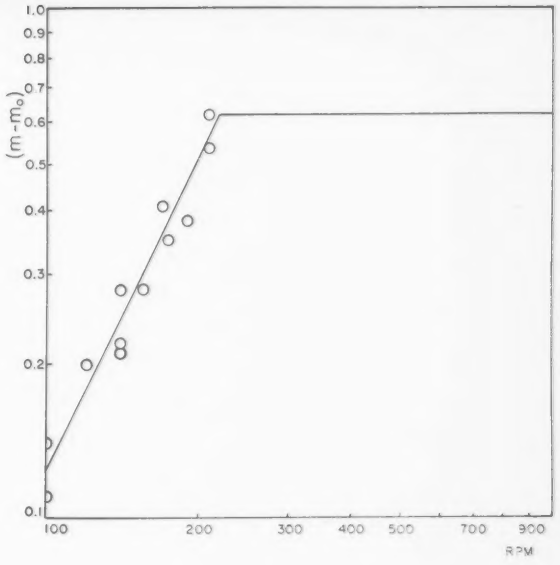

Figure 11—Effective volume of mixing vs. agitator speed.

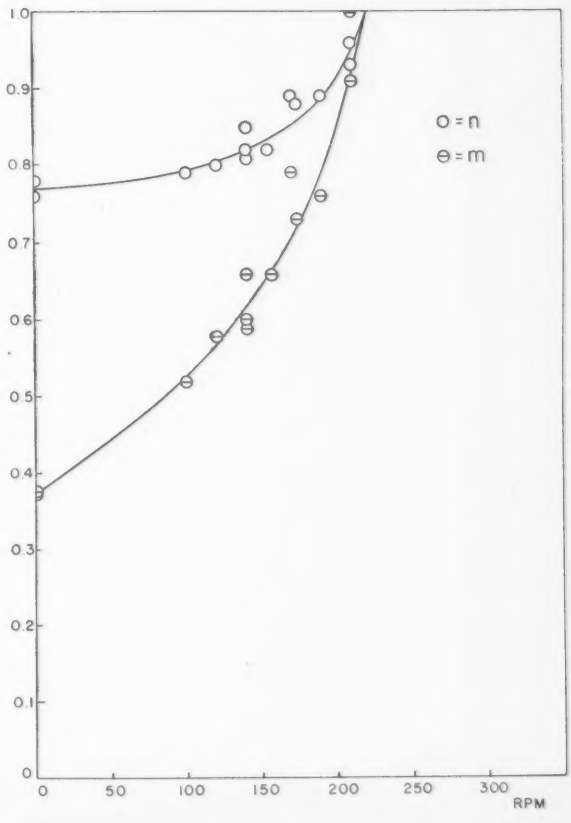

Figure 13—Variation of m and n with agitator speed.

straight lines drawn through the experimental points at different levels of agitation, for values of agitator r.p.m., designated as N, ranging from 0 to 210. Values of m and n were determined from them for each agitator speed by the method described.

Even at an r.p.m. of 0 given values of m and n were obtained; they were designated as m_o and n_o. For any given value of N, then, the value of $m - m_o$ might represent the contribution of the agitator r.p.m. to the level of mixing.

It has been found that when plotting $(m - m_o)$ vs N on log-log paper, as shown in Figure 11, a straight line of slope 2 is obtained which can be represented by the equation:

$$m - m_o = a\,N^2$$

For the particular system studied, the constants m_o and a were found to be 0.38 and 1.25×10^{-5} respectively.

The value of 0.38 for m_o indicates the level of mixing obtained when the agitator is at rest, through the agitation produced by the introduction of the feed. Such an effect appears to have been mentioned first by MacDonald and Piret [16], when measuring mixing times in a vessel.

As the value of m reaches 1, when the agitator speed is increased, a maximum value of $(m - m_o)$ is reached. This value remains constant thereafter even if the agitator speed is increased because the system behaves as one giving perfect mixing.

Proceeding in a similar way, the values of $(n - n_o)$ vs N were plotted on log-log paper as shown in Figure 12, giving a straight line of slope 3. The values of n are thus related to the agitator r.p.m. by the equation:

$$n - n_o = b\,N^3$$

where, for the particular system studied, $n_o = 0.77$ and $b = 2 \times 10^{-8}$.

When plotting, on a linear scale, the values of m and n as a function of N, as in Figure 13, both variables are found to reach a maximum value of 1 at an r.p.m. of approximately 220, indicating that the system behaves then as one giving perfect mixing.

Conclusions

The method described to determine mixing efficiencies in continuous flow systems should prove to be a very useful tool in evaluating the actual performance of mixers. Not only is it possible to obtain optimum results with a given mixer but the relative performance of mixers of different design can be established since efficiency measurements are possible.

The contribution to the design of tank flow reactors should also be of importance because a method is now available to take into account the effects of partial mixing. Improved designs, with the best possible use of agitators, should result.

The experimental results obtained to date are very promising. While they do not draw a complete picture as yet, due to the limited extent of experimental work which could be performed, they point to a number of investigations which should lead to a comprehensive knowledge of mixing.

A new experimental set-up providing for a wider variety of investigations is nearing completion. Among others, the factors to be studied include the position, speed of rotation, shape and size of the agitator, the physical properties and the relative depth of the liquid, the location of the feed, the manner in which it is introduced, its rate and inlet velocity, and the outlet position relative to the inlet.

Other types of agitating systems will be considered, including those with internal recirculation and of the draft-tube type.

The study of systems involving chemical reactions is already under way.

Nomenclature

a = Constant, relating effective volume to agitator speed.
b = Constant, relating short-circuit effect to agitator speed.
c = Volumetric concentration, lbs./ft.^{3}
  c_F : concentration of the feed.
  c_M : concentration of the effluent if mixing was perfect, when a chemical reaction is present.
  c_o : initial concentration.
  c' : concentration in the zone of perfect mixing.
K, K_1, K_1', K_2, K_3 : Constants of integration.
m = Fraction of the total volume which is perfectly mixed.
  m_o : value of m when the agitator is at rest.
n = Fraction of the feed entering the zone of perfect mixing.
  n_o : value of n when the agitator is at rest.
N = Agitator speed, R.P.M.
p = Fraction of the feed going to the stagnant zone.
q = Rate of flow, ft.^{3}/hr.
r = Reaction rate, lbs./(ft.^{3}) (hr.)
s = Fraction of part nq of the feed entering the zone of perfect mixing which subsequently passes out into the stagnant zone.
t = Time, hrs.
  $t_1 : \dfrac{(1 - m)V}{nsq}$
V = Volume, ft.^{3}

References

(1) Coulson and Richardson, Chemical Engineering, Vol. II, p. 917, McGraw Hill Co. (1955).
(2) Perry, J. H., Chemical Engineers' Handbook, 3rd Ed., p. 1195, McGraw Hill Co. (1950).
(3) Rushton, J. H., Ind. Eng. Chem. 45, 93 (1953).
(4) Rushton, J. H., Ind. Eng. Chem. 46, 133 (1954).
(5) Rushton, J. H., Ind. Eng. Chem. 47, 582 (1955).
(6) Rushton, J. H., Ind. Eng. Chem. 48, 552 (1956).
(7) McCabe and Smith, Unit Operations of Chemical Engineering, p. 292, McGraw Hill Co. (1956).
(8) MacMullin, R. B., and Weber, H., Trans. A.I.Ch.E. 31, 409 (1935).
(9) Denbigh, K. G., Trans. Faraday Soc. 40, 352 (1944).
(10) Weber, A. P., Chem. Eng. Prog. 49, 26 (1953).
(11) Colburn, A. P., Trans. A.I.Ch.E. 31, 457 (1935).
(12) MacMullin, R. B., Chem. Eng. Prog. 49, 33 (1953).
(13) Beaudry, J. P., Chem. & Met. Engr. 55 No. 7, 112 (1948).
(14) Danckwerts, P. V., Chem. Eng. Sci. 2, 1-13 (1953).
(15) Germain, J. E., Bull. Soc. Chim. France (1957) 484-5.
(16) MacDonald, R. W., and Piret, E. L., Chem. Eng. Prog. 47, 363 (1951).
(17) Nagata, S., Eguchi, W., Inamura, R., Tanigawa, K., and Tanaka, T., Chem. Eng. (Japan) 17, 387 (1953).
(18) Nagata, S., Eguchi, W., and Tanaka, T., Chem. Eng. (Japan) 19, 163 (1955).
(19) Suzuki, E., and Saito, J., Chem. Eng. (Japan) 21, 91 (1957).
(20) Smith, J. M., Chemical Engineering Kinetics, p. 172, 175, McGraw Hill Co. (1956).

★ ★ ★

Sodium Hydroxide-Sodium Sulphate Stripping of Uranium from Amine Extracts[1]

A. I. BELLINGHAM[2] and R. SIMARD[3]

Batch shake-out tests on two tertiary amines and one secondary amine to determine the effects of sodium sulphate concentration and pH on the distribution of uranium between 0.1N amine in kerosene and aqueous sodium sulphate solution showed that transfer of uranium from the solvent to the aqueous phase was favored by increasing pH values up to 5.5 and by increasing the aqueous sodium sulphate concentration up to 20% w/v Na_2SO_4.

Continuous counter-current stripping of tri-iso-octylamine (TIOA) extracts with 20% w/v Na_2SO_4 was also carried out in a three-stage mixer-settler arrangement in which the pH was controlled by the addition of 10% NaOH to the three stages. Further addition of caustic to the separated aqueous strip solution to raise the pH to 7.0-7.2 yielded a high grade uranium precipitate (88% U_3O_8). The continuous testing confirmed the results of the shake-out tests and showed that the procedure gave results comparing favorably with other stripping methods accompanied by a lower overall reagent cost.

AMINE solvent extraction of uranium from sulphuric acid solutions produced in the leaching of ores has been the subject of much investigation in the last few years. At the U.S.A.E.C., Oak Ridge National Laboratory, in particular, K. B. Brown, D. J. Crouse and others have made extended studies [1] of long chain amines which have proven to be efficient extractants for uranium.

The amine solvent extraction is best explained by an ion exchange mechanism which may be represented as follows:

$$(R_3NH)_2SO_4 + [UO_2(SO_4)_2]^{=} \rightleftharpoons (R_3NH)_2 \cdot UO_2(SO_4)_2 + SO_4^{=}$$

It is well known that the loaded amine extracts can be stripped by a similar exchange using acidified solutions of chloride or nitrate salts, or with sodium carbonate, ammonium carbonate and alkalis which react irreversibly as neutralizing agents.

In the course of studies being made on the application of solvent extraction to the hydrometallurgy of Canadian uranium ores, work relating to the use of certain amines, has shown that the loaded extract can also be stripped effectively by sodium sulphate solutions at a controlled pH favouring uranium in the aqueous phase. This led to an investigation of continuous counter-current stripping which has been incorporated in a pilot plant flowsheet.

In this work, three amines were investigated by small scale batch testing. These were (1) tertiary tri-iso-octyl amine supplied by Carbide Chemical Company, Montreal, Que., (2) a tertiary amine labelled C_8-C_{10} mixture supplied by General Mills, Inc., Kankakee, Ill., (3) a secondary dodecenyl amine labelled 9D-178 supplied by Rohm and Haas Company of Canada Limited, West Hill, Ont. In the batch testing all three products responded favorably to stripping with sodium sulphate solution. However, since the tri-iso-octyl amine, at the time the work was done, appeared to have some advantages over the other two in the extraction section of the process, it was chosen for the continuous testing.

Procedure

Batch cross-current stripping was done in open beakers with mechanical stirrers using 250 ml. of 0.1N amine (in kerosene) which had been previously saturated by contact with uranyl sulphate solutions at pH 1.4-1.5. Three or four 50-ml. fractions of sodium sulphate solution were contacted successively with the extract. For each stage of stripping 10% NaOH was used to obtain the required pH at equilibrium. The strip fractions were separated after each stage in a separatory funnel and assayed for U_3O_8. The final stripped solvent was also assayed for U_3O_8.

Two main variables to be studied were Na_2SO_4 concentration and pH. The uranium distribution curves, Co vs. Ca expressed as U_3O_8 g/l in organic and aqueous, were plotted as a function of pH and sulphate concentrations. From these data it was possible to predict the feasibility of an efficient continuous stripping circuit using three counter-current stages at a controlled pH. This was incorporated in a bench-scale extraction unit already treating uranium leach solutions.

Results

A. Batch cross-current stripping

Equilibrium data are represented graphically in Figures 1, 2 and 3. The pH as shown in Figure 1 was found to be a critical variable. For efficient stripping or for less than 0.1 g U_3O_8/1 in the solvent, the pH should be controlled at 4.5 to 5.0. Higher pH values will cause local precipitation in the first stage where uranium concentration is high (15-20 g U_3O_8/1).

[1] *Manuscript received January 8, 1959.*

[2] *Present address: South Australia, Department of Mines.*

[3] *Scientific Officer, Radioactivity Division, Mines Branch, Ottawa, Ont.*

Published by permission of the Director, Mines Branch, Department of Mines and Technical Surveys, Ottawa, Ont.

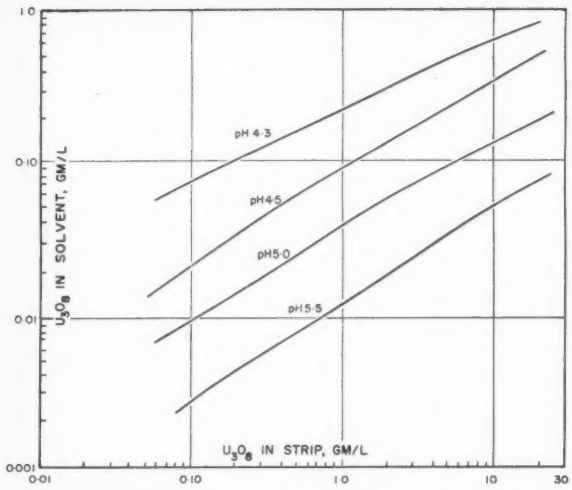

Figure 1—Distribution curves. O.1N tri-iso-octyl amine vs 20% w/v Na_2SO_4 Effect of pH.

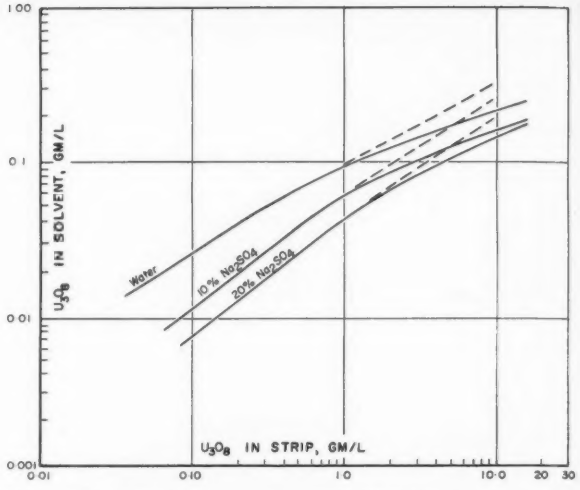

Figure 2 — Distribution curves. O.1N tri-iso-octyl amine strip at pH Effect of Na_2SO_4 concentration.

The effect of varying the sodium sulphate concentration is illustrated in Figues 2 and 4 for 0.1N TIOA (Tri-iso-octylamine). In Figure 2 the dotted lines would represent the true equilibrium if no sulphate were picked up in the first cross-current stage. At this stage, for a volume ratio of solvent to strip of 5 to 1, the Na_2SO_4 increase in the strip is approximately 3%, so that the curves for water, 10% and 20% of Na_2SO_4, are in fact, 3%, 13% and 23% Na_2SO_4 respectively. This explains the apparent dip in the curves of Figure 2. The data from the corrected curves of Figure 2 were used to plot the distribution coefficients of Figure 4.

In view of the results obtained with tri-iso-octylamine, other amine extractants were studied. Equilibrium data for Rohm and Haas secondary amine 9D-178 and for General Mills tertiary amine C_8-C_{10} are represented in Figure 3.

B. Continuous counter-current tests

To confirm the equilibrium data obtained from batch testing, a series of continuous extraction and stripping runs was carried out in a small pilot plant extraction unit designed to test various leach solutions obtained from the treatment of Canadian uranium ores.

The flow diagram is shown in Figure 5. Figure 6 is a detailed sketch of the 4-stage mixer-settler unit currently used for extraction. The three-stage stripping unit is a scale-down of the extractor. The two units operating in a closed organic circuit were designed for a throughput of 400-600 ml. feed solution per minute. Loaded extract from the extractor flows counter-currently to a stream of Na_2SO_4 solution through three mixer-settlers. The pH of the aqueous phase in the first mixer is controlled from a pH recorder-controller which actuates the sodium hydroxide valve. Stage 2 and 3 are controlled manually to maintain the set pH as read by a Beckman pH meter.

The operating conditions and results of a number of continuous runs are shown in Table 1. Data from run 532 were used to establish the operating equilibria of Figure 7.

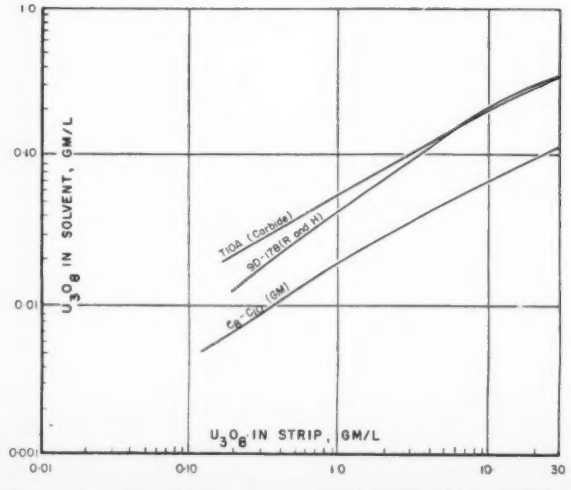

Figure 3 — Distribution curves. pH 4.75-20% w/v Na_2SO_4.

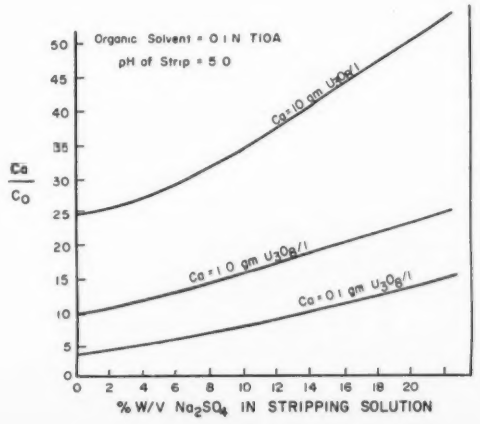

Figure 4—Effect of Na_2SO_4 concentration on distribution coefficient.

TABLE 1

CONTINUOUS EXTRACTION AND STRIPPING TESTS
OPERATING CONDITIONS AND RESULTS

Run No.	529	530	531	532
Flows ml/min —				
Pregnant Feed Solution	550	305	308	365
Organic: 0.1N TIOA,	186	100	120	120
Strip Solution: 20% w/v Na_2SO_4	57	38	48	52
Assays				
Pregnant Solution, pH	1.60	1.60	1.60	1.60
" " U_3O_8 gm/l	1.73	1.73	1.73	1.81
Raffinate Stage 1 " "	1.75	1.74	0.47	0.98
" " 2 " "	1.85	1.11	0.007	0.028
" " 3 " "	1.12	0.052	<0.001	0.001
" " 4 " "	0.075	0.002	<0.001	<0.001
Organic Extract " "	5.15	5.32	5.01	5.46
Strip Stage 1 " "	13.75	14.51	11.48	12.30
" " 2 " "	5.39	3.35	0.59	2.92
" " 3 " "	1.98	0.68	0.14	0.41
Recycle Solvent " "	0.48	0.14	0.03	0.03
Average operating pH of				
Strip Stage 1	4.4	4.5	4.6	4.75
" " 2	4.2	4.6	4.5	4.80
" " 3	4.2	4.5	4.9	4.80
NaOH Consumed For strip control and precipitation lb NaOH/lb U_3O_8	1.1	0.9	1.0	1.2
Precipitate Assay U_3O_8%	80.5	84.2	89.7	89.5

From the above table and from Figure 7, it can be seen that theoretical equilibrium conditions can be approached in continuous operation. The pH control did not prove as difficult as anticipated. After some preliminary experience, the automatic pH meter could be made to control at a pH of 4.7+-0.15 which is satisfactory for an on-off controller. At times there was some slight precipitation of uranium due to localized high pH at the point of addition, but it redissolved and no trouble was experienced. The phase separation in the strippers was rapid with the primary break occurring in 50 seconds. In the mixing step of the stripping operation, the minimum retention time so far used has been 5 minutes per stage and has been adequate.

The precipitation of uranium from the sulphate strip

TABLE 2

COMPARATIVE RESULTS OF VARIOUS STRIPPING METHODS

Strip Solution	Reagent Consumption lb./lb. U_3O_8	Precipitate Grade % U_3O_8	Recycle Barren Strip Treatment
Sodium Sulphate 20% Na_2SO_4 NaOH precipitation	NaOH–1.0	85–88	None
Sodium Chloride 1.0M NaCl 0.05M H_2SO_4 NaOH precipitation	NaCl–3.0 H_2SO_4–0.25 NaOH–0.70	85	Removal of excess sodium sulphate by crystallization
Sodium Carbonate 10% Na_2CO_3 NaOH precipitation	NaOH–1.30		Removal of excess sodium sulphate by crystallization and conversion of excess NaOH to carbonate using a carbonation tower.

by adding NaOH to pH 7.0-7.2 produced a high-grade product that could be settled readily and filtered well. The filtering rate on the settled portion was estimated at 5 lb. dry precipitate per sq. ft. per hour.

Reagent consumption for stripping and precipitation in all tests was close to 1 lb. NaOH per lb. U_3O_8 and this confirms the theoretical consumption based on the U_3O_8/SO_4 ratio in the extract. From the assays of the extract the mol ratio in the solvent is close to 3 SO_4 to 1 U. On this basis, complete neutralization to pH 7.0 would be as represented in the following reaction:

$$2\,(R_3NH)_4 \cdot UO_2(SO_4)_3 + 14\,NaOH \longrightarrow 8\,R_3N + Na_2U_2O_7 + 6\,Na_2SO_4 + 11\,H_2O$$

or 21 mols NaOH per mol U_3O_8

or close to 21 x 40/842 = approximately 1 lb. NaOH/lb.U_3O_8

A simple explanation for the mechanism of sulphate stripping at controlled pH has been to assume that the uranyl ion forms a double salt with Na_2SO_4 thus depressing the activity of the anion complex $[UO_2(SO_4)_3]^{-4}$.

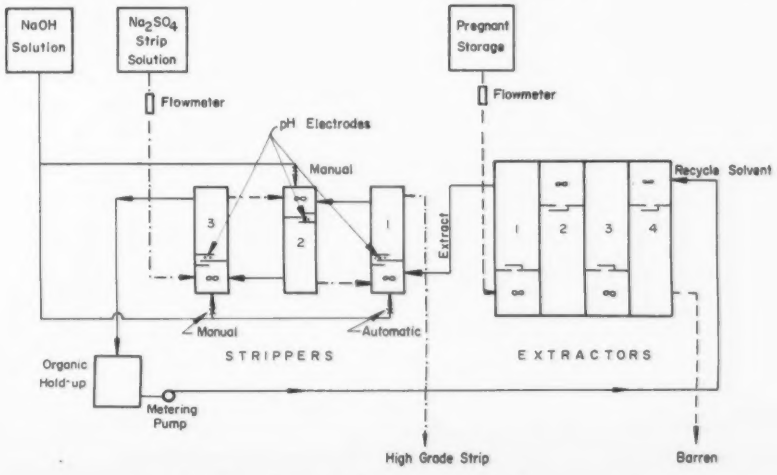

Figure 5—Flow diagram. Extraction and sulphate stripping using TIOA.

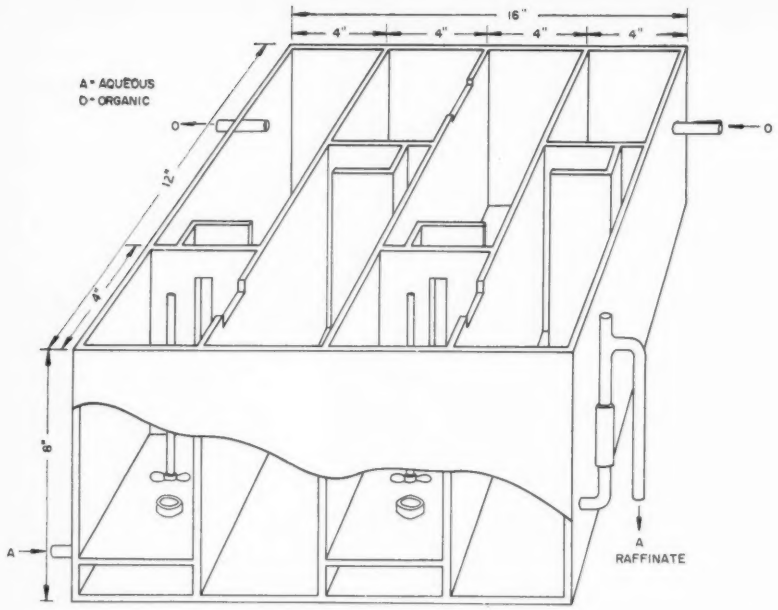

Figure 6—Four stage mixer settler (¼" lucite).

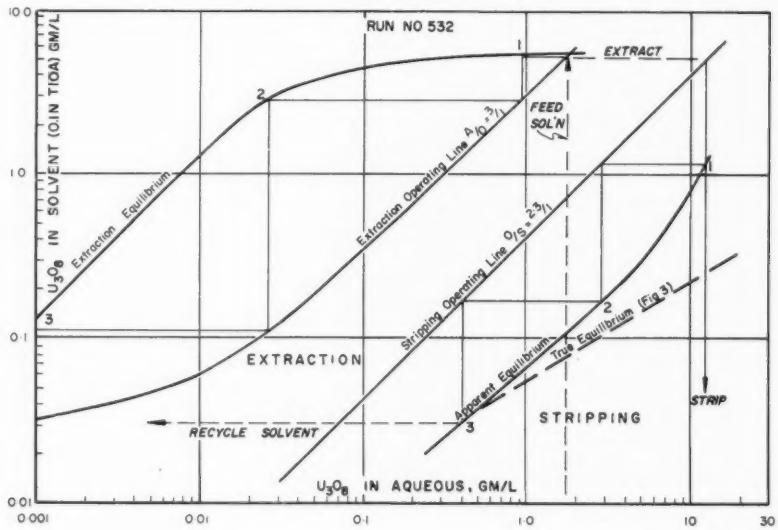

Figure 7—Graphical representation of continuous counter-current extraction and stripping.

Conclusion

The results of the test work reported here were sufficiently encouraging for the process to be tested on several uranium bearing solutions from the leaching of various ores. This additional work confirmed the work described in this paper [2, 3, 4] and demonstrated that sodium sulphate stripping of uranium from amine extractants was simpler and cheaper than by chloride or carbonate solutions. The method is simpler in that the barren strip solution may be recycled directly without any form of regeneration or purification whereas other strip solutions must be retreated before recycling. The sulphate strip process, however, would necessitate more stringent pH control and instrumentation than other stripping methods. Table 2 shows a comparison of three common methods for stripping uranium from amine extracts.

Nomenclature

Ca = concentration U_3O_8 g/1 in aqueous solution
Co = concentration U_3O_8 g/1 in organic solution
$\frac{Ca}{Co}$ = distribution coefficient
A = aqueous feed solution flowrate, ml/min
O = organic solvent
S = aqueous stripping solution flowrate, ml/min

References

(1) Brown, K. B., Crouse, D. J., Coleman, C. F., "Some New Solvent Extraction Processes for Use in the Hydrometallurgical Treatment of Uranium, Thorium and Vanadium Ores". Paper presented at the A.I.M.E. meeting, New Orleans, February 25-28, 1957.
(2) Simard, R., "Recovery of Uranium and Thorium from Solution Ref. No. 5/57-8 by Amine Solvent Extraction". TR 145/57, Radioactivity Division, Mines Branch, Ottawa.
(3) Bellingham, A., Simard, R., "Recovery of Uranium from Rexspar Leach Solution by Solvent Extraction with Tri-Iso-Octyl Amine". SR-46/57, Radioactivity Division, Mines Branch, Ottawa.
(4) Simard, R., "Solvent Extraction for the Recovery of Uranium and Thorium from Leach Solutions of a Uranium Ore (Ref. 7/57-7) from the Bancroft Area, Ontario. IR 58-4, Radioactivity Divisions, Mines Branch, Ottawa.

★ ★ ★

A Note on Thermodynamic Consistency of Ternary Vapor-Liquid Equilibrium Data[1]

JAMES C. M. LI[2] and BENJAMIN C.-Y. LU[3]

Graphical and numerical integration methods are proposed for testing the thermodynamic consistency of ternary vapor-liquid equilibrium data, in which the integration of the Gibbs-Duhem equation can be performed under isothermal and isobaric conditions. No data-fitting procedure is involved in the proposed methods, therefore the uncertainty as to whether the deviations are due to experimental errors or to the inadequacy of the employed equation can be avoided. When one part of the data is less precise than the others, the proposed method may be employed to detect the inconsistent part.

THERMODYNAMIC consistency has been the most reliable test of vapor-liquid equilibrium data. Especially for the ternary systems, the experimental difficulties involved are such that a preliminary set of data has to be tested against thermodynamic consistency before one can even trust his experimental technique. In the literature, many test methods have been proposed. The experimental data are tested either by fitting them with some integrated forms of the Gibbs-Duhem equation, or by graphical integration of the Gibbs-Duhem equation along a particular path. When data fitting procedure is involved, using equations such as those proposed by Benedict et al. (1) and Wohl (2), the uncertainty as to whether the deviations are due to experimental errors or to the inadequacy of the employed equation can not be avoided. Methods which involve graphical integration along a particular path may also encounter practical difficulties. Recently Herrington (3) has suggested two methods, one of which involves integration of the Gibbs-Duhem equation along a line parallel to one of the bases of the triangular coordinates, thus keeping the mole fraction of one component constant. The other method, which modifies the method of Colburn and Schoenborn (4), involves integration of the Gibbs-Duhem equation along a straight line connecting one of the vertices to a point in the opposite base. In this method, the ratio of two of the mole fractions is kept constant. He also proved that these methods are applicable to systems with more than one liquid phase, provided that the whole liquid is treated as a single phase by using the overall mole fractions and activity coefficients, etc. The integration can therefore actually go through the two liquid phase region without any discontinuity. The purpose of keeping one of the mole fractions or the ratio of two of the mole fractions constant is to simplify the integration of the Gibbs-Duhem equation. However, to restrict some relation among the mole fractions has several disadvantages:

1. Since most of the vapor-liquid equilibrium data are measured at constant pressure, a restriction in the mole fraction will force the integration to go through a non-isothermal region, to which, strictly speaking, the Gibbs-Duhem equation derived from isothermal and isobaric conditions cannot be applied.

2. Unless the experimental points lie exactly on the straight line required for these methods, some interpolation or extrapolation may be involved which will cause additional uncertainty.

3. These methods may not go through the region of more reliable or more abundant data at ease without sometimes covering some undesirable region.

The purpose of this investigation is to introduce a method in which the integration of the Gibbs-Duhem equation can be performed along any curve in the triangular coordinates, especially along the curve of constant temperature and pressure where the method is thermodynamically exact.

Integration of the Gibbs-Duhem equation

Under isothermal and isobaric conditions, the Gibbs-Duhem equation for a ternary liquid solution may be expressed as

$$x_1 \, d \log \gamma_1 + x_2 \, d \log \gamma_2 + x_3 \, d \log \gamma_3 = 0 \quad \text{(at T,p)} \ldots (1)$$

where x_1, x_2 and x_3 are the liquid mole fractions of components 1, 2 and 3 respectively, and γ_1, γ_2 and γ_3 are the liquid activity coefficients of components 1, 2

[1]*Manuscript received September 27, 1958.*
[2]*Present Address: Fundamental Research Laboratory, U.S. Steel Corporation, Monroeville, Pa. Home address: 297 Jerry Lane.*
[3]*Department of Chemical Engineering, University of Ottawa, Ottawa,*
Based on a paper presented at the 41st Annual Conference, C.I.C., Toronto, Ont, May 26-28, 1958.

and 3 respectively, using pure liquids as standard states. The Scatchard's excess free energy of mixing may be expressed in the form [5]

$$Q = x_1 \log \gamma_1 + x_2 \log \gamma_2 + x_3 \log \gamma_3 \quad (\text{at T,p}) \ldots\ldots (2)$$

Then, it is seen

$$dQ = \log \gamma_1 \, d\, x_1 + \log \gamma_2 \, d\, x_2 + \log \gamma_3 \, d\, x_3 \quad (\text{at T,p}) \ldots (3)$$

Since $Q = 0$ at the three vertices of the triangular coordinates, an integration of Equation (3) along a curve connecting two of the vertices will give

$$\int_{x_1=0}^{x_1=0} \log \gamma_1 \, d\, x_1 + \int_{x_2=0}^{x_2=0} \log \gamma_2 \, d\, x_2 + \int_{x_3=0}^{x_3=0} \log \gamma_3 \, d\, x_3 = 0 \ldots\ldots (4)$$

Equation (4) may be applied to ternary vapor-liquid equilibrium data obtained under isobaric conditions, provided that the change of temperature along the curve is not large. For exact correlations, the integration can be performed along the curve of constant boiling temperatures, which gives

$$Q_b - Q_a = \int_a^b \log \gamma_1 \, dx_1 + \int_a^b \log \gamma_2 \, dx_2 + \int_a^b \log \gamma_3 \, dx_3 \quad (\text{at T,p}) \ldots (5)$$

where a and b are any two points on the same curve. The problem is now how to evaluate these integrals. A direct method (Method 1) would be integrating each of the integrals graphically. This can be done by plotting $\log \gamma_1$ against x_1, $\log \gamma_2$ against x_2 and $\log \gamma_3$ against x_3. The points have to be taken from the curve in the triangular coordinates in the sequence from point a to point b. The same sequence has to be used in each plot. Since

$$dx_1 + dx_2 + dx_3 = 0$$

$$Q_b - Q_a = \int_a^b \log \frac{\gamma_1}{\gamma_3} \, dx_1 + \int_a^b \log \frac{\gamma_2}{\gamma_3} \, dx_2 \ldots\ldots\ldots (6)$$

Therefore, only two plots, namely $\log (\gamma_1/\gamma_3)$ against x_1 and $\log (\gamma_2/\gamma_3)$ against x_2 will be necessary. If a and b coincide to one point, that is if the integration is taken along a closed curve, or a and b are two of the vertices, then the value of the sum of the integrals is zero. A somewhat similar approach has been proposed by Broughton and Brearley [6] for testing isobaric data. However, instead of testing data along constant temperature curves, they assumed that the product T log γ is independent of temperature. The validity of this assumption seems questionable even for binary systems [7].

In some instances, calculations using relative volatilities are more advantageous than using the activity coefficients. If the integration is along the curve of constant boiling temperature and if the vapor phase can be assumed ideal, Equation (5) becomes

$$\Delta \left(x_1 \log \frac{y_1}{x_1} + x_2 \log \frac{y_2}{x_2} + x_3 \log \frac{y_3}{x_3} \right) = \int_a^b \log \alpha_{13} \, dx_1 + \int_a^b \log \alpha_{23} \, dx_2 \ldots\ldots\ldots (7)$$

where α_{13}, α_{23} are the relative volatilities defined by

$$\alpha_{13} = \frac{y_1}{x_1} \Big/ \frac{y_3}{x_3}$$

$$\alpha_{23} = \frac{y_2}{x_2} \Big/ \frac{y_3}{x_3} \ldots\ldots\ldots\ldots\ldots\ldots (8)$$

and Δ is the difference of the quantity in the parentheses between the points a and b. Should the curve be a straight line, the ratio of dx_1: dx_2: dx_3 is a constant, only one integration is needed. In this case the right-hand side of Equation (6) becomes,

$$\int_a^b \left[\log \frac{\gamma_1}{\gamma_3} + \frac{x_{2b} - x_{2a}}{x_{1b} - x_{1a}} \cdot \log \frac{\gamma_2}{\gamma_3} \right] dx_1 \ldots\ldots\ldots\ldots (9)$$

The evaluation of the integrals of Equation (5) may also be carried out by means of a numerical integration (Method 2). This method has the advantage that it can be applied to almost any set of data without using any graphical procedure, provided that the experimental points are reasonably spaced. Let the points be a, 1, 2, . . . 9, b. Assuming that all the curves of log γ against x can be approximated by segments of straight lines connecting the points, the first integral of Equation (5) can be calculated by

$$\int_a^b \log \gamma_1 \, dx_1 = \frac{1}{2} \Big[(\log \gamma_{1a} + \log \gamma_{11}) (x_{11} - x_{1a}) + (\log \gamma_{11} + \log \gamma_{12}) \cdot (x_{12} - x_{11}) + \ldots \Big]$$

$$= \frac{1}{2} \Big[x_{1b} \log \gamma_{1b} \cdot \gamma_{19} - x_{1a} \log \gamma_{1a} \cdot \gamma_{11} + x_{11} \log (\gamma_{1a}/\gamma_{12}) + x_{12} \log (\gamma_{11}/\gamma_{13}) + \ldots + x_{19} \log (\gamma_{18}/\gamma_{1b}) \Big] \ldots\ldots (10)$$

where x_{1a} is the mole fraction of component 1 at point a, γ_{1a} is the activity coefficient of component 1 at point a, etc. Similar expressions may be obtained for the second and the third integrals. Combining these expressions together with the Quantities Q_a and Q_b, which are defined by Equation (2), the following equation is obtained:

$$x_{1a} \log \left(\frac{\gamma_{1a}}{\gamma_{11}} \right) + x_{11} \log \left(\frac{\gamma_{1a}}{\gamma_{12}} \right) + x_{12} \log \left(\frac{\gamma_{11}}{\gamma_{12}} \right) + \ldots +$$

$$x_{19} \log \left(\frac{\gamma_{1b}}{\gamma_{1b}} \right) + x_{1b} \log \left(\frac{\gamma_{19}}{\gamma_{1b}} \right) + x_{2a} \log \left(\frac{\gamma_{2a}}{\gamma_{21}} \right) + x_{21} \log \left(\frac{\gamma_{2a}}{\gamma_{22}} \right) +$$

$$x_{22} \log \left(\frac{\gamma_{21}}{\gamma_{23}} \right) + \ldots + x_{29} \log \left(\frac{\gamma_{28}}{\gamma_{2b}} \right) + x_{2b} \log \left(\frac{\gamma_{29}}{\gamma_{2b}} \right) +$$

$$x_{3a} \log \left(\frac{\gamma_{3a}}{\gamma_{31}} \right) + x_{31} \log \left(\frac{\gamma_{3a}}{\gamma_{32}} \right) + x_{32} \log \left(\frac{\gamma_{31}}{\gamma_{33}} \right) + \ldots +$$

$$x_{39} \log \left(\frac{\gamma_{38}}{\gamma_{3b}} \right) + x_{3b} \log \left(\frac{\gamma_{39}}{\gamma_{3b}} \right) = 0 \ldots\ldots (11)$$

This summation is simply that for each component, multiply the mole fraction at any point with the logarithm of the ratio of the activity coefficients of a point preceding it and of a point following it, except the first and last points, where the activity coefficient of its own is used if there is no point preceding it or if there is no point following it. It is convenient to tabulate the calculation as shown in Table 1.

If a and b coincide to one point, that is, if the curve is closed, then every point has a point preceding it and

TABLE 1

ACETONE-METHANOL-WATER AT 100°C. (4)

Run No.	x_1	$\log \gamma_1$	$x_1 (\log \gamma_{1p} - \log \gamma_{1f})$	x_2	$\log \gamma_2$	$x_2 (\log \gamma_{2p} - \log \gamma_{2f})$	x_3	$\log \gamma_3$	$x_3 (\log \gamma_{3p} - \log \gamma_{3f})$
29	0.215	0.4082	−0.01406	0.033	0.0398	+0.00316	0.752	0.0792	−0.00136
31	0.158	0.4736	−0.01506	0.088	−0.0560	+0.00200	0.754	0.0810	+0.00054
33	0.119	0.5035	−0.01297	0.119	0.0170	−0.00536	0.762	0.0785	−0.00137
35	0.089	0.5826	−0.01604	0.131	−0.0110	−0.00665	0.780	0.0828	+0.01533
38	0.066	0.6230	−0.00283	0.119	0.0678	−0.01747	0.815	0.0588	+0.03632
39	0.028	0.6255	+0.00088	0.182	0.1358	−0.00888	0.790	0.0382	+0.01533
37	0.033	0.5917	+0.00378	0.204	0.1166	−0.00590	0.763	0.0394	−0.02258
36	0.043	0.5110	+0.00336	0.225	0.1069	+0.01140	0.732	0.0678	−0.02938
34	0.069	0.5136	+0.00128	0.198	0.0660	+0.01486	0.733	0.0795	−0.02082
32	0.100	0.4925	+0.00211	0.193	0.0318	+0.00659	0.707	0.0962	−0.01179

$\Sigma + = 0.12284$
$\Sigma - = 0.18122$
Total = − 0.05838
% Deviation = 38.4%

Repeat the above calculation without run Nos. 29, 31 and 33

$\Sigma + = 0.12051$
$\Sigma - = 0.12767$
Total = − 0.00716
% Deviation = 5.8%

a point following it. The summation is to be performed as if every point is a point inside a curve. Experimental data over the entire concentration range may be conveniently divided into several small sets and the thermodynamic consistency can be tested on each of them. In doing so, the less reliable region may be easily spotted. If one of the experimental points is much in error in a set of data, it may be singled out by successively including the experimental point, one by one, in a set.

An example of this calculation is shown in Table 1, where the data for the ternary system, acetone-methanol-water at 100°C. [8] are tested. The values of the activity coefficients are taken directly from the original article [8]. These activity coefficients are the thermodynamic activity coefficients for the liquid, and are not based on assuming an ideal gaseous solution in vapor phase. Since the pressure effect on liquid activity coefficients is usually small, it is neglected in this calculation. For the ten experimental points (Nos. 29, 31, 33, 35, 38, 39, 37, 36, 34 and 32) which form a curve as indicated on the triangular diagram (Figure 1), the overall deviation in thermodynamic consistency is about 38%, while the experimental points in the middle of the triangular diagram (Nos. 14, 17, 16, 18, 21, 23, 26, 28, 30, 25, 24, 20 and 19) indicate a deviation of 10%. The deviation is defined as

$$\frac{/(\Sigma +) + (\Sigma -)/}{(\Sigma +) - (\Sigma -)} \times 100$$
$$2$$

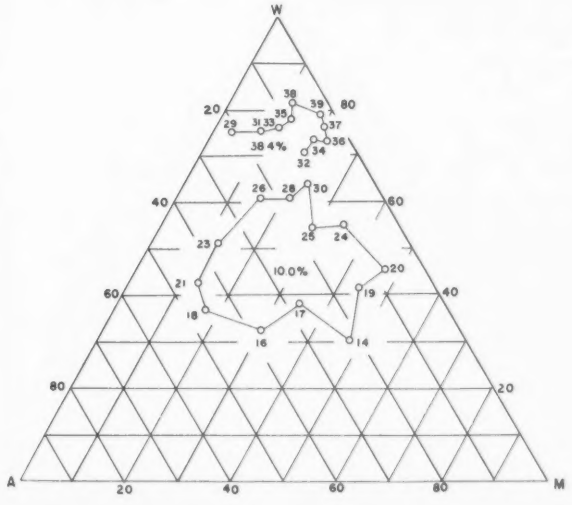

Figure 1 — Thermodynamic consistency of vapor-liquid equilibrium data for the system acetone-methanol-water at 100°C.[8]. Percentages indicated are overall deviations.

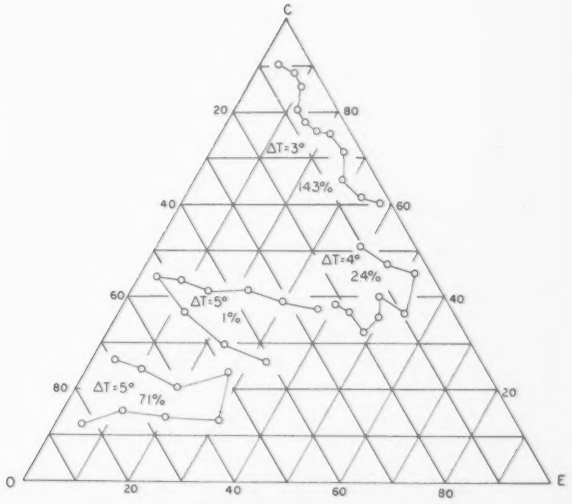

Figure 2 — Thermodynamic consistency of vapor-liquid equilibrium data for the system n-octane-ethylbenzene-cellosolve at 760 mm. Hg. pressure [9]. Percentages indicated are overall deviations.

It is obvious that the consistency of the data in the middle of the triangular diagram is better than the consistency of the points Nos. 29 . . . 32. If the calculation as shown in Table 1 is repeated, excluding the experimental points Nos. 29, 31 and 33, the % deviation reduces to 6%. It is seen that these points seem to be inconsistent.

The application of the numerical integration method to a ternary system at constant pressure is shown in Figure 2, in which the data of the system n-octane-ethyl benzene–cellosolve [9] are tested. The experimental points are grouped in such a way that the boiling point differences are kept at a minimum. It is seen that the deviations are not uniform throughout the whole concentration range. The experimental data on high cellosolve concentrations seem to be less consistent than the data of low cellosolve concentrations.

Although this numerical integration method is sufficiently accurate for experimental data of average precision in most cases, it can only be reliable if the points are not too few and are close enough to warrant the segmental line approximation of the log γ vs. x curves. For fewer and widely separated points, a better approximation which utilizes the parabola approximation of any set of three consecutive points may be used (Method 3). This is similar to the Simpson's method of numerical integration. For data of very high precision, this method is also needed to detect any less precise points.

For any set of three consecutive points, say x_{11}, x_{12} and x_{13} (mole fractions of component 1 at points 1, 2 and 3 respectively) with values of log γ_{11}, log γ_{12} and log γ_{13}, if a parabola is drawn to pass them, the area under the curve of log γ against x is equal to

$$\int_1^3 \log \gamma_1 \, dx_1 = \frac{1}{2}(x_{13} - x_{11}) \log \gamma_{13}\gamma_{11} - \frac{1}{6}(x_{13} - x_{11})^2 \cdot \left[\frac{\log (\gamma_{13}/\gamma_{12})}{x_{13} - x_{12}} - \frac{\log (\gamma_{12}/\gamma_{11})}{x_{12} - x_{11}} \right] \quad \ldots(12)$$

Similar expressions may be obtained for the second and third integrals of Equation (5). In Equation (12) the first term on the right hand side is similar to that of Equation (10). Therefore, the second term serves as a correction to the second method and the order of magnitude compared to the overall summation of Equation (11) will indicate whether the third method is necessary or not. In a practical calculation, this method requires a set of odd number of experimental points. The sum of all the integrals should add up to $(Q_b - Q_a)$ for any set of points which constitute a curve in the triangular coordinates.

Still more accurate numerical method does not seem to warrant discussion. Only some points of interest will be mentioned here. First, since it is not necessary to restrict any relation between the mole fractions, the integration does not have to go through a multi-liquid phase region where there are almost no actual experimental data. The integration can stop at a point on the saturation curve or go through along a tie line. The integration along a tie line is not necessary since the terminal Q values can be easily calculated. Instead, it is recommended to integrate along the saturation curve where the experimental data are usually available. Second, it is customary to plot the vapor-liquid equilibria on a triangular coordinate paper using the vapor composition, y, of one of the components as parameter. In this case, the Gibbs-Duhem equation can be modified to become:

$$d \log p_1^\circ = x_2 \, d \log \frac{p_1^\circ y_2}{p_2^\circ} + x_3 \, d \log \frac{p_1^\circ y_3}{p_3^\circ} \quad \ldots\ldots(13)$$

where the vapor phase is assumed ideal and the vapor composition of component 1 is a constant. Integration of Equation (13) along the line of constant y_1 will be further simplified if the temperature variation is small:

$$\int_a^b x_2 \, d \log y_2 + \int_a^b x_3 \, d \log y_3 = 0 \quad \ldots\ldots(14)$$

Numerical integration can be performed using either the second or the third method by tabulating x_2 versus log y_2 and x_3 versus log y_3.

References

(1) Benedict, M., Johnson, C. A., Solomon, E., and Rubin, L. C., Trans. A.I.Ch.E. 41, 371 (1945).
(2) Wohl, K., Trans. A.I.Ch.E. 42, 215 (1946).
(3) Herrington, E. F. G., Research (London) 3, 41 (1950); J. Appl. Chem. (London) 2, 11 (1952), 2, 19 (1952).
(4) Colburn, A. P., and Schoenborn, E. M., Trans. A.I.Ch.E. 41, 221 (1945).
(5) Redlich, O., and Kister, A. T., Ind. Eng. Chem. 40, 375 (1948).
(6) Broughton, D. B., and Brearley, C. S., Ind. Eng. Chem. 47, 838 (1955).
(7) Yu, K.-T., and Coull, James, Chem. Eng. Progress Symposium Ser. 48, No. 2, 38 (1952).
(8) Griswold, John, and Wong, S. Y., Chem. Eng. Progress Symposium Ser. 48, No. 3, 18 (1952).
(9) Murti, P. S., and van Winkle, Matthew, A.I.Ch.E. Journal 3, 517 (1957).

★ ★ ★

Some Thermodynamic Properties of the System Formic Acid-Water[1]

A. C. PLEWES[2], *D. C. PEI*[3] *and R. K. CODE*[4]

The integral latent heats of vaporization of formic acid-water mixtures at 760 mm. Hg. are reported and used to prepare an enthalpy-concentration chart for the system. The data provided a basis for the estimation of the heats of mixing in the vapor phase, and the results indicate that the exothermic heat of mixing may be attributed to the partial dimerization of monomeric formic acid coupled with the association of water and acid molecules.

Vapor-liquid equilibria data for the system are also reported.

THIS paper is one of a series [1, 2] reporting the results of studies carried out at Queen's University on the properties of liquid mixtures in an effort to obtain useful data for industrial design projects and to explain the behavior of two unlike molecules in homogeneous solution. The experimental work involved the measurement of the integral latent heats of vaporization of formic acid-water mixtures. Vapor-liquid equilibria data at 760 mm.Hg. were also obtained as complete temperature-composition data were required in the preparation of an enthalpy-concentration chart. The previously reported equilibria data of Othmer [3] could not be used as no temperatures were recorded and the data were obtained at an average total pressure of 750 mm.Hg. Similar studies of acid-water systems involving other homologous organic acids are being continued.

Experimental equipment and procedure

The experimental heats of vaporization were obtained in a modified version of a calorimeter used by Dana [4]. The calorimeter (Figure 1) is composed of a heater, C, and a silvered, evacuated Dewar flask, B. B is surrounded by a concentric glass cylinder, S, which is sealed to the top of the Dewar flask. Liquid from a constant head device enters S through Y and is boiled at a controlled pressure of 760 mg.Hg. The chamber, S, is connected to a reflux condenser at R. Solution at the bubble point enters A through the capillary, D, in the base of the Dewar flask. The solution entering A is evaporated as quickly as it enters, thus ensuring evaporation at constant composition. The vapor produced in chamber A is withdrawn through the sidearm N, condensed, and retained for future sampling and analysis. The vessel, S, is heated externally by a chromel heating element imbedded in insulation and acts as a preheater for the liquid feed. Heat transfer between chamber A and the surroundings is reduced to a negligible amount by the evacuated Dewar flask and chamber S. For the system formic acid-water the maximum temperature difference at steady state between chambers A and S was less than two centigrade degrees. The heater, C, consists of an electrical resistance element immersed in a bath of high-boiling silicone oil. The resistance element and bath are completely enclosed in a glass tube. With this modification in the original calorimeter design corrosive liquids may be studied.

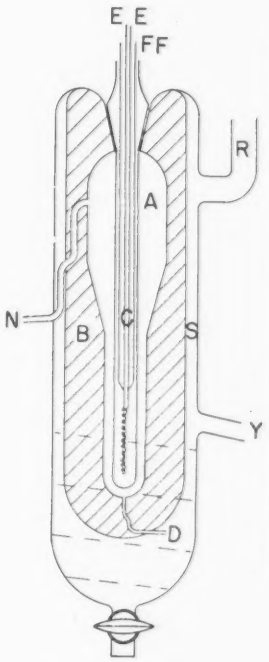

Figure 1—Calorimeter.

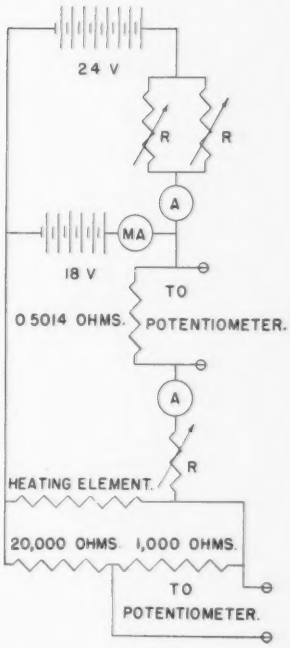

Figure 2—Electrical circuit.

A diagram of the electrical circuit is shown in Figure 2. A 24-volt battery served as a power source and was connected in parallel with an 18-volt battery as ballast. This arrangement reduced the current fluctuations in the heater. The specific gravity of the battery electrolyte was kept within the range 1.20-1.30. The current was obtained from measurements of the potential drop across

[1]*Manuscript received December 19, 1958.*
[2]*Head, Department of Chemical Engineering, Queen's University, Kingston, Ont.*
[3]*Graduate student, Division of Chemistry and Chemical Engineering, California Institute of Technology, Pasadena, Calif.*
[4]*Assistant Professor, Department of Chemical Engineering, Queen's University, Kingston, Ont.*
Contribution from the Department of Chemical Engineering, Queen's University, Kingston, Ont.

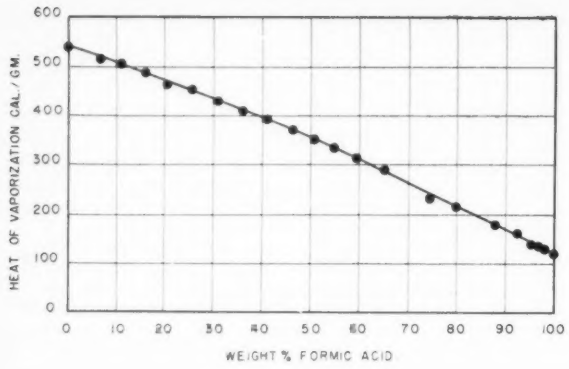

Figure 3—Integral heats of vaporization of formic acid-water mixtures.

a standard resistance of 0.5014 ohms. Two 10,000 ohm and one 1,000 ohm standard resistances, connected in parallel with the heating element, were used for voltage measurement. With this arrangement the power input to the heating element could be measured within ± 0.2%.

The vapor-liquid equilibria data were obtained in a still designed by Ellis [5]. Ellis has tested this still for a number of binary mixtures involving both high and low activity coefficient systems composed of close and wide boiling components and compared the results with those obtained in stills of the Othmer, Fenske and Gillespie types. On the basis of activity coefficient tests he has shown that better experimental data are obtained with this new design.

Analytical formic acid (90 wt.% acid) was obtained from the British Drug Houses and distilled in a column packed with ¼ in. glass helices to a depth of five feet. The operation of the column at atmospheric pressure and a reflux ratio of 20:1 gave a middle third distillate of 99.6 wt.% acid. This material was subsequently frozen and distilled under vacuum at room temperature to remove the residual water. The density of the final product was 1.2218 gm./ml. at 20°C. Once distilled city water was used without further treatment.

The condensate samples were titrated with 0.1N barium hydroxide protected from atmospheric carbon dioxide. Phenolphthalein was used as an indicator.

The calorimeter was tested by measuring the heats of vaporization of formic acid and water at 760 mm.Hg. The mean value of three determinations of the heat of vaporization of the purified formic acid was 118.0 cal./gm. A value of 117.8 cal./gm. for 100% acid was obtained by extrapolation of the heats of vaporization for acid-water mixtures ranging from 92.5 to 99.6 wt.% acid. A value of 120.0 cal./gm. obtained by Brown is given in the International Critical Tables [6]. An experimental value of 115.4 cal./gm. is reported by Coolidge [7]. Using the Clapeyron equation and his experimental vapor pressure and vapor and liquid density data Coolidge estimated a value of 114.0 cal./gm. A value of 115.6 cal./gm. is listed in Circular 500 of the National Bureau of Standards [8]. It is believed that the data reported in this paper are more accurate than the values just listed. This opinion is prompted by the design and operational details of the calorimeter and on the fact that the extrapolated value of 117.8 cal./gm. checked the results obtained with purified formic acid. The experimental heat of vaporization of water was 539.3 cal./gm. which checks with the value of 539.4 cal./gm. given by Keenan and Keyes [9].

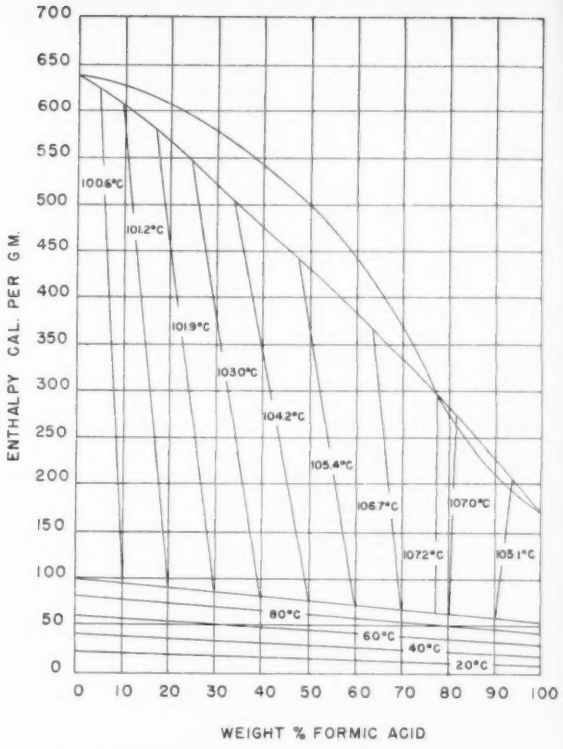

Figure 4 — Enthalpy-concentration chart for the system formic acid-water at 760 mm. Hg.

The isobaric integral heats of vaporization of formic acid-water mixtures were obtained over the entire range of concentrations. Two runs were made at each concentration and an average value is reported. Runs were continued for a period of one to two hours to ensure steady state operation during the experimental measurements. The criterion for steady state was the constancy and similarity of feed and distillate compositions. The calorimeter was operated at a boil-up rate of 3-5 gm./min. in Chamber A. At this boil-up rate there was no entrainment and a determination could be made in a reasonable time.

The vapor-liquid equilibria data were obtained by operation of the Ellis still for periods of two hours. A second series of thirty-minute runs was carried out in the 90-100 wt.% acid range when it was discovered that formic acid tended to decompose when mixtures of high acid content were subjected to prolonged refluxing. The decomposition was found to be negligible if the refluxing time was less than one hour. The still was tested with the system acetic acid-water to see if equilibrium conditions could be reached in thirty minutes. The data obtained checked well with published values [10]. According to Ellis [5] 20-30 minutes is sufficient time to reach equilibrium.

Experimental results and discussion

Enthalpy-concentration data for the system formic acid-water are presented in Table 1 and Figures 3 and 4. The integral heats of vaporization listed in Table 1 were read from the smoothed curve through the experimental data of Figure 3. The specific heat and heat of solution data for formic acid-water mixtures reported by Glagoleva [11, 12] and the temperature-composition data and

integral heats of vaporization obtained experimentally in this study were used in the preparation of the enthalpy-concentration chart (Figure 4).

TABLE 1

ENTHALPY-CONCENTRATION DATA FOR THE SYSTEM FORMIC ACID-WATER AT 760 MM. HG.

Composition, wt. % acid	Integral Heat of Vaporization, cal./gm.	Enthalpy of Saturated Liquid, cal./gm.	Enthalpy of Saturated Vapor, cal./gm.
0	539.3	100.0	639.3
10	509.4	95.5	604.9
20	473.8	91.0	564.8
30	436.1	86.4	522.5
40	396.2	81.9	478.1
50	355.7	77.4	433.1
60	312.5	72.8	385.3
70	265.6	68.3	333.9
80	220.0	63.7	283.7
90	172.8	58.8	231.6
100	118.0	53.8	171.8

The enthalpy of each pure component, in the liquid state, was assumed to be zero at 0°C. The datum level for liquid formic acid was chosen as 4.226 cal./gm. at 8.3°C. and 760 mm.Hg. This corresponds to an enthalpy of zero for liquid formic acid at 0°C. and 760 mm.Hg. as the normal freezing point of formic acid is 8.3°C. Vapor-liquid equilibria data for the system are also included in the enthalpy-concentration chart.

Liquid isotherms were estimated at 20 degree intervals using the heat of solution and specific heat data. The saturated liquid line was drawn so that it intersected the liquid isotherms at known temperatures and compositions. The saturated vapor line was located by adding the integral heat of vaporization at constant pressure to the enthalpies of the liquid line. Isotherms in the vapor region are not included in the enthalpy-concentration chart due to the lack of experimental heats of mixing in the vapor phase.

In the final phase of the study the heats of mixing of formic acid and water in the vapor phase were estimated. The results provided information on the possible structure of the vapor and reasons for the departure of the system from an ideal solution. The procedure used was similar to that described in detail in a previous paper for the system acetic-acid water [2]. The method is reviewed briefly as follows:

(1) The heats of mixing were estimated from the difference between the actual enthalpies and the ideal enthalpies for various mixtures. The ideal enthalpy of a mixture was obtained by the addition of the enthalpies of the pure components at the ideal conditions of zero pressure and the temperature of the system.

(2) The variation of enthalpy of the pure components with pressure was obtained by graphical integration of the thermodynamic relationship [13]:

$$\Delta H = H_p - H_{p^\circ} = \int_{p^\circ}^{p} \left[V - T\left(\frac{\delta V}{\delta T}\right)_p \right] dp \qquad \ldots\ldots(1)$$

The ideal enthalpies of water vapor were estimated by extrapolation of the data in the steam tables [9] to zero pressure. In the case of formic acid the change in enthalpy with pressure was determined down to 25 mm.Hg. by graphical integration of Equation (1) using the P-V-T data of Coolidge [14]. From 25 mm.Hg. to zero pressure it was assumed that the acid vapor was composed of monomer and dimer, and that any resulting enthalpy change was due to association or dissociation reactions. Thus,

$$\Delta H = H_{25\text{mm.Hg.}} - H_{p^\circ} = \alpha \Delta H_R$$

where

ΔH_R = molal heat of the association reaction
α = fraction of monomer dimerized at equilibrium

$$HCOOH \rightleftharpoons \frac{1}{2}(HCOOH)_2$$

$$K_p = \frac{(p_{dimer})^{1/2}}{p_{monomer}} \text{ or } K_p^2 = \frac{p_{dimer}}{(p_{monomer})^2}$$

$$K_p^2 = \frac{\frac{\alpha/2}{1-\alpha/2} P}{\left(\frac{1-\alpha}{1-\alpha/2}\right)^2 P^2} = \frac{\alpha/2\,(1-\alpha/2)}{(1-\alpha)^2 P}$$

and

$$\alpha = 1 \pm \sqrt{\frac{1}{4PK_p^2 + 1}}$$

where

P = total pressure

$$\Delta H = \alpha \Delta H_R = \left[1 - \sqrt{\frac{1}{4PK_p^2 + 1}} \right] \Delta H_R \qquad \ldots\ldots(2)$$

since

$$\alpha \leq 1$$

The change in enthalpy due to the dimerization reaction was evaluated using Equation (2) and the heats of dimerization and equilibrium constants determined by Waring [13]. The total change in enthalpy with pressure for formic acid was then obtained from the sum of Equations (1) and (2) and the results are presented in Table 2.

The estimated heats of mixing and dimerization are compared in Figure 5 and Table 2. The heat of mixing in the vapor phase is exothermic and approximately 90% of this heat effect may be attributed to the dimerization reaction. At low acid concentrations the difference between the heat of mixing and the heat effect due to dimerization is small and increases with acid concentration to a maximum in the region of the azeotrope (77.4 wt.% acid). This increase is believed to be due to the association of formic acid and water molecules. If it is assumed that the heat of mixing is due to (1) the heat of association of formic acid monomer to dimer and (2) the heat of association of formic acid and water molecules, the structures of the associated molecules in the vapor phase may be pictured as follows:

Formic Acid Dimer

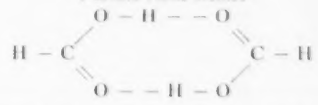

Associated Formic Acid-Water Molecule

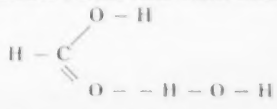

From the above structures it is evident that the heat effect per associated molecule for the dimerization reaction is approximately twice that for the formic acid-water asso-

TABLE 2

HEATS OF MIXING OF FORMIC ACID-WATER MIXTURES IN THE VAPOR PHASE AT 760 MM. HG.

Composition, wt. % acid	Enthalpy of Water Vapor (zero pressure and dewpoint), cal./gm.	Enthalpy of Formic Acid Vapor (zero pressure and dewpoint), cal./gm.	Enthalpy of Vapor Mixture (zero pressure and dewpoint), cal./gm.	Enthalpy of Vapor Mixture (760 mm. Hg. and dewpoint), cal./gm.	Heat of Mixing	
					$H_{latm.} - H_{p=o}$, cal./gm.	Heat of Dimerization, cal./gm.
0	642.9	–	642.9	639.3	−3.6	0
10	643.5	287.0	607.9	604.9	−3.0	−2.6
20	644.1	288.0	572.9	564.8	−8.1	−7.0
30	644.5	288.7	537.8	522.5	−15.3	−13.7
40	644.9	289.5	502.7	478.1	−24.6	−22.0
50	645.3	290.4	467.9	433.1	−34.8	−31.8
60	645.7	291.3	433.1	385.3	−47.8	−42.3
70	646.0	291.8	398.1	333.9	−64.2	−54.2
80	645.9	291.8	362.6	283.7	−78.9	−68.1
90	645.5	291.0	326.5	231.6	−94.9	−86.0
100	–	286.1	286.1	171.8	−114.3	−110.7

ciation. Unfortunately, there is no direct means of estimating the heat effect due to the association of formic acid and water molecules in the vapor phase. Other associated structures are possible, e.g. water with formic acid dimer, but the degree of association in more complicated structures than those considered should be quite small and the corresponding heat effects negligible.

Vapor-liquid equilibria data required in the construction of the enthalpy-concentration chart are presented as supplementary material in Table 3 and Figure 6. At 760 mm.Hg. the system forms a maximum boiling azeotrope at 77.4 wt.% formic acid and 107.2°C. in agreement with the data of Minjer and Reinders reported by Horsley [16]. Two sets of data were obtained as formic acid tends to decompose when mixtures of high acid content are subjected to prolonged refluxing. The first

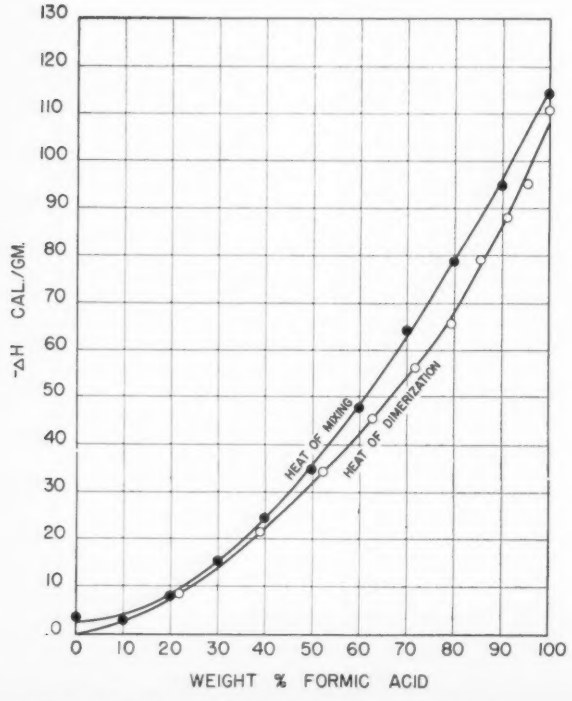

Figure 5—Heats of mixing in the vapor phase.

TABLE 3

VAPOR-LIQUID EQUILIBRIA DATA FOR THE SYSTEM FORMIC ACID-WATER AT 760 MM. HG.

Temperature, °C.	x, Mole Fraction Acid in Liquid Phase	y, Mole Fraction Acid in Vapor Phase
Refluxing Time: 2 hr.		
101.0	0.047	0.020
101.6	0.098	0.047
102.1	0.156	0.082
103.4	0.223	0.124
104.1	0.281	0.174
105.5	0.370	0.268
106.0	0.412	0.332
107.1	0.567	0.552
107.2	0.573	0.573
106.4	0.674	0.733
105.0	0.792	0.853
104.8*	0.794	0.847
103.8	0.843	0.908
102.7	0.901	0.952
101.7	0.948	0.978
Refluxing Time: ½ hr.		
105.2	0.768	0.839
104.8*	0.794	0.851
103.5*	0.857	0.920
103.0	0.882	0.944
102.5	0.913	0.962
100.9	0.962	0.989

*Estimated by graphical interpolation

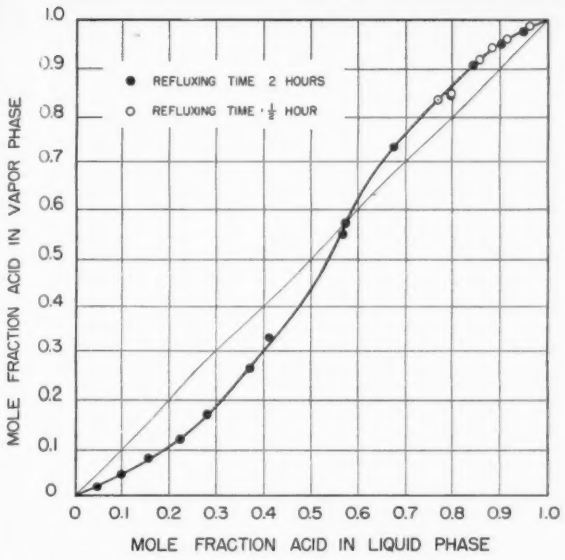

Figure 6—x-y diagram for the system formic acid-water at 760 mm. Hg.

set covering a complete range of acid concentration was obtained at a refluxing time of two hours. A second set was obtained at a shorter refluxing time of thirty minutes in the concentration range of 90-100 wt.% acid. The effect of refluxing time on formic acid decomposition is illustrated in Table 4.

Acknowledgement

This study was made possible through the award of a R. S. McLaughlin Fellowship to one of the authors (D.C.P.).

TABLE 4

THE EFFECT OF REFLUXING TIME ON FORMIC ACID DECOMPOSITION

Refluxing Time, hours	Liquid Composition, wt. % acid	Vapor Composition, wt. % acid
0.5	90.8	93.6
1.0	90.8	93.6
2.0	90.7	93.4
3.0	90.8	93.3
5.0	90.6	93.0
7.0	90.0	92.6

References

(1) Plewes, A. C., Jardine, D. A., and Butler, R. M., Can. J. Tech. 32, 133 (1954).
(2) Plewes, A. C., Butler, R. M., and Pugi, K., Can. J. Tech. 34, 152 (1956).
(3) Othmer, D. F., Ind. Eng. Chem. 4, 232 (1932).
(4) Dana, L. I., Proc. Am. Acad. Arts Sci. 60, 241 (1925).
(5) Ellis, S. R. M., Trans. Inst. Chem. Engrs. 30, 58 (1952).
(6) International Critical Tables, Vol. V, p. 136, McGraw-Hill Book Company, New York, 1927.
(7) Coolidge, A. S., J. Am. Chem. Soc. 52, 1874 (1930).
(8) Rossini, F. D., et al, "Selected Values of Chemical Thermodynamic Properties", Circular 500, National Bureau of Standards, Washington, D.C.
(9) Keenan, J. H., and Keyes, F. G., "Thermodynamic Properties of Steam", John Wiley and Sons, Inc., New York, 1936.
(10) Gilmont, R., and Othmer, D. F., Ind. Eng. Chem. 36, 1061 (1944).
(11) Glagoleva, A. A., J. Gen. Chem. (U.S.S.R.) 11, 768 (1941).
(12) Glagoleva, A. A., and Cherlar, S. I., J. Gen. Chem. (U.S.S.R.) 6, 685 (1936).
(13) Hougen, O. A., and Watson, K. M., "Chemical Process Principles", p. 493, John Wiley and Sons, Inc., New York, 1947.
(14) Coolidge, A. S., J. Am. Chem. Soc. 50, 2166 (1928).
(15) Waring, W., Chem. Revs. 51, 171 (1952).
(16) Horsley, L. H., "Azeotropic Data", p. 6, A.C.S., Washington, 1952.

★ ★ ★

LETTERS TO THE EDITOR

Menlo Park, California.

Editor, C.J.Ch.E.:

RE: The Effect of the Less Viscous Liquid in the Laminar Flow of Two Immiscible Liquids by T. W. F. Russell and M. E. Charles published in the February 1959 issue of C.J.Ch.E.

This paper brings to mind some unpublished work which L. R. Handley and the writer did in 1952 and which culminated in U.S. Patent 2,821,205 of January 1958.

At the time, we were considering means of reducing the pressure drop of pipe lines pumping extremely highly viscous crude oil. By means of injecting a thin film of water at the pipe wall, we were able to accomplish the effect which is so well illustrated in the paper by Messrs. Russell and Charles.

In order to minimize the amounts of water to be handled and the chance that this water might emulsify with oil, we restricted ourselves to amounts of water less than 2% of the crude oil pumped. It is interesting to note that in a laboratory installation with over 50 feet of approximately 1-inch pipe there appeared to be no mixing of oil and water and substantially the entire water film could be removed intact at the terminal of the line.

Two problems became apparent for the practical application of this method in long crude oil pipe lines. The first is the necessity for cleaning the pipe so thoroughly that all traces of oil are removed from the pipe wall and then treating this wall in such a way that it will remain water-wet. If this is done successfully, even temporary stoppages of the water flow will not cause oil to wet the wall, and the water film can be re-established with ease. But except for new clean lines, the process necessary to remove all traces of oil is extremely tedious and expensive.

The second problem is concerned with the difference in specific gravity between oil and water. Fortunately, this difference is seldom great, and highly viscous crude oils tend to be closer to the gravity of water than less viscous ones. Nevertheless, in long lines there will be a tendency to thin the annular layer of water on one side of the pipe, to thicken it on the other, and thereby reduce the efficiency of the process. If the difference in the specific gravity of the fluids is very small, that of the water could be economically adjusted by the admixture of other fluids.

It may be of interest to note that if the water film is very thin compared to the diameter of the pipe and when the viscosity of the oil is very large compared to that of water one can visualize the oil as flowing like a solid plug lubricated by the water film in the pipe. Moreover, it is a fair assumption in this case that the velocity in the water film varies nearly linearly from zero at the wall to that of the plug at the interface. In this case the thickness of the water film divided by the pipe diameter will be approximately $\frac{1}{2}$ the ratio of the quantity of water pumped to that of oil. This can be verified by dividing Equation 22 by Equation 21 in the paper and using the assumptions made above.

E. G. Chilton,
Stanford Research Institute.

Edmonton, Alta.

Editor, C.J.Ch.E.:

We thank Dr. Chilton for his comments and agree that the relation $\frac{Qw}{Qo} = \frac{r_o - r}{r_o}$; (using the nomenclature of the original paper) is approximately valid for plug flow under the conditions he describes.

Dr. Chilton mentions that the wetting characteristics of the pipeline wall and the density differential between oil and water phases are two of the problems to be considered in the commercial application of the concentric flow system. Current pilot pipeline investigations at the Research Council of Alberta with oil and water phases of equal density indicate that for a given oil there is a region of stable concentric flow provided the pipe is maintained in a water-wet condition.

M. E. Charles and T. W. F. Russell,
Research Council of Alberta.

The Canadian Journal of Chemical Engineering

formerly

Canadian Journal of Technology

INSTRUCTIONS TO AUTHORS

Manuscript Requirements

1. The manuscript should be in English or French.
2. The original and two copies of the manuscript should be supplied. These are to be on 8½ x 11 inch sheets, typewritten, and double spaced. Each page should be numbered.
3. Symbols should conform to American Standards Association. An abridged set of acceptable symbols is found in the third edition of Perry's Chemical Engineers' Handbook. Greek letters and subscripts and superscripts should be carefully made.
4. Abstracts of not more than 200 words in English indicating the scope of the work and the principal findings should accompany all technical papers.
5. References should be listed in the order in which they occur in the paper, after the text, using the form shown here: "Othmer, D. F., Jacobs, Jr., J. J., and Levy, J. F., Ind. Eng. Chem. 34, 286 (1942). Abbreviations of journal names should conform to the "List of Periodicals Abstracted by Chemical Abstracts". Abbreviations of the common journals are to be found in Perry's Handbook also. All references should be carefully checked with the original article.
6. Tables should be numbered in Arabic numerals. They should have brief descriptive titles and should be appended to the paper. Column headings should be brief. Tables should contain a minimum of descriptive material.
7. All figures should be numbered from 1 up, in Arabic numerals. Drawings should be carefully made with India ink on white drawing paper or tracing linen. All lines should be of sufficient thickness to reproduce well, especially if the figure is to be reduced. Letters and numerals should be carefully and neatly made, preferably with a stencil. Generally speaking, originals should not be more than twice the size of the desired reproduction; final engravings being 3¼ in. or 7 in. wide depending on whether one column or two is used.
8. Photographs should be made on glossy paper with strong contrasts. Photographs or groups of photographs should not be larger than three times the size of the desired reproduction.
9. All tables and figures should be referred to in the text.

Submission of Manuscripts

1. The three copies of the manuscript, including figures and tables, should be sent directly to:

   DR. A. CHOLETTE, editor,
   The Canadian Journal of Chemical Engineering,
   Faculty of Science, Laval University,
   Boulevard de l'Entente,
   Quebec, Que.
2. The authors addresses and titles should be submitted with the manuscript.
3. The author may suggest names of reviewers for his article, but the selection of the reviewers will be the responsibility of the editor. Each paper or article is to be reviewed by two chemical engineers familiar with the topic. Reviewers may request that they remain anonymous.
4. All correspondence regarding reviews should be directed to the editor.

Reprints

1. At least 50 free "tear sheets" of each paper will be supplied.
2. Additional reprints may be purchased at cost. An estimated cost of reprints, with an attached order form, will be sent to the author with the galley proofs.
3. Orders for reprints must be made before the paper has appeared in the Journal.

* * *